

THE CANADIAN MINERALOGIST

Volume 40

August 2002

Part 4

The Canadian Mineralogist
Vol. 40, pp. 1025-1046 (2002)

THE SOURCE OF BASALT VESSELS IN ANCIENT EGYPTIAN ARCHEOLOGICAL SITES: A MINERALOGICAL APPROACH

LEANNE M. MALLORY-GREENOUGH[§]

*Department of Earth and Environmental Sciences, Okanagan University College, 3333 College Way,
Kelowna, British Columbia V1V 1V7, Canada*

MICHAEL P. GORTON

Department of Geology, University of Toronto, 22 Russell Street, Toronto, Ontario M5S 3B1, Canada

JOHN D. GREENOUGH

*Department of Earth and Environmental Sciences, Okanagan University College, 3333 College Way,
Kelowna, British Columbia V1V 1V7, Canada*

ABSTRACT

Basalt vessels are rare, but ubiquitous items in elite Predynastic (4000–3100 BCE) and First Dynasty (3100–2800 BCE) Egyptian burials. Where the bedrock sources can be identified, these artefacts can be used to study trade and social interaction between communities before the advent of writing. Seven Egyptian, post-Jurassic (unaltered), alkali and tholeiitic basalt units, representing all likely sources, were multiply sampled, and augite, plagioclase, pigeonite (tholeiites), and olivine analyzed (~1000 electron-microprobe analyses) in each sample. Flows can be distinguished using combinations of major and minor constituents from individual minerals (*e.g.*, Al₂O₃ versus SiO₂ in plagioclase or augite, and FeO versus SiO₂ in olivine). However, plots of the composition of coexisting minerals (*e.g.*, CaO/(CaO + Na₂O + K₂O)_{Plagioclase} versus CaO/(CaO + MgO + FeO)_{Augite} or MgO/(MgO + FeO)_{Olivine}; K₂O/FeO_{Plagioclase} versus MnO/TiO₂_{Augite}, or K₂O/(CaO + Na₂O + K₂O)_{Plagioclase} versus SiO₂/TiO₂_{Olivine}) and multidimensional scaling applied to augite and plagioclase indicate that multi-mineral discrimination of units is more effective than single-mineral discrimination. Discriminant analysis (multivariate analysis of variance) shows that units can be efficiently distinguished using multi-mineral data, although single minerals also provide effective discrimination. Furthermore, the combination of TiO₂, FeO and CaO in augite, and SiO₂, Al₂O₃ and Na₂O in plagioclase, discriminates between Egyptian alkaline and tholeiitic basalts as well as do the whole-rock data. Approximately 2700 electron-microprobe analyses of minerals in microsamples (1 mg) from 117 Egyptian basalt vessels indicate, unequivocally, that the bedrock source of every vessel is the Haddadin lava flow in northern Egypt. During the Predynastic period, the trade in basalt vessels was probably controlled from Maadi, the settlement closest to the Haddadin flow and richest in recycled “factory seconds”.

Keywords: mineral geochemistry, basalt discrimination, archeology, Egypt, artefacts, Predynastic, basalt vessels.

[§] E-mail address: jdgreeno@ouc.bc.ca

SOMMAIRE

Les vaisseaux de basalte sont rares mais assez répandus dans les sites d'enterrement de l'élite égyptienne à l'ère Prédynastique (4000–3100 avant l'ère chrétienne) et de la Première Dynastie (3100–2800 avant l'ère chrétienne). Dans les cas où la source du basalte peut être identifiée, ces artefacts peuvent servir à étudier les tracés d'échanges commerciaux et les interactions sociales entre communautés avant l'introduction des documents écrits. Sept unités basaltiques post-Jurassiques non altérées, comprenant basaltes alcalins et tholéitiques, et représentant toutes les sources possibles de ces vaisseaux, ont été échantillonnées afin d'étudier l'augite, le plagioclase, la pigeonite (tholéïtes), et l'olivine (~1000 analyses à la microsonde électronique des minéraux dans chaque échantillon). On parvient à distinguer les coulées en utilisant une combinaison des constituants majeurs et mineurs des minéraux individuels, par exemple Al_2O_3 versus SiO_2 dans le plagioclase ou l'augite, et FeO versus SiO_2 dans l'olivine. Toutefois, les groupements de données sur la composition de minéraux coexistants, par exemple $CaO/(CaO + Na_2O + K_2O)_{\text{Plagioclase}}$ versus $CaO/(CaO + MgO + FeO)_{\text{Augite}}$ ou $MgO/(MgO + FeO)_{\text{Olivine}}$, $K_2O/FeO_{\text{Plagioclase}}$ versus $MnO/TiO_2_{\text{Augite}}$, ou $K_2O/(CaO + Na_2O + K_2O)_{\text{Plagioclase}}$ versus $SiO_2/TiO_2_{\text{Olivine}}$, évalués par normalisation multidimensionnelle telle qu'appliquée à l'augite et au plagioclase, indiquent qu'une discrimination des unités fondée sur plusieurs minéraux est plus révélatrice qu'une discrimination fondée sur un seul minéral. D'après une analyse multivariable de la variance, on peut effectivement distinguer les unités de basalte en utilisant les données sur plusieurs minéraux, quoique les minéraux considérés seuls donnent aussi de bons résultats. De plus, une combinaison de TiO_2 , FeO et CaO dans l'augite, et de SiO_2 , Al_2O_3 et Na_2O dans le plagioclase, sert à distinguer entre basaltes égyptiens alcalins et tholéitiques aussi bien que les compositions globales des roches. Environ 2700 analyses à la microsonde électronique de micro-échantillons (1 mg) de 117 vaisseaux égyptiens faits de basalte montre sans équivoque que c'est le basalte de la coulée de Haddadin, dans le nord de l'Égypte, qui serait la source dans chaque cas. Au cours de l'ère Prédynastique, le commerce des vaisseaux de basalte était probablement sous le contrôle de Maadi, le centre habité le plus près de la coulée de Haddadin et le plus riche en pièces de second choix recyclées.

(Traduit par la Rédaction)

Mots-clés: géochimie des minéraux, discrimination des basaltes, archéologie, Égypte, artefacts, ère Prédynastique, vaisseaux de basalte.

INTRODUCTION

Rock materials are ubiquitous in archeological artefacts. In some cases, petrological descriptions of these materials can be used to identify their geological sources. Locating the source provides trade and cultural information. For many rock types (*e.g.*, basalts), simple petrographic descriptions provide useful (Lucas 1930, Williams 1983, Porat & Seeher 1988) but non-definitive information about source. On the other hand, geochemical data on whole rocks and constituent minerals have much to offer archeologists (Mallory-Greenough *et al.* 2000). For example, with geochemical discrimination based on whole-rock major-element and trace-element geochemistry, it is possible to place the rocks in a geological context (Irvine & Baragar 1971, Pearce & Cann 1973, Winchester & Floyd 1977, Pearce 1996). Depending on grain size, these methods may require significant amounts of sample (100 g to >10 kg) in order to obtain representative samples. With outcrops as sample sources, this has not been a major issue. In archeology, of course, priceless artefacts cannot be pulverized, and sample size and sampling technique become crucial.

Our experiments indicate that mineral compositions shows much promise as indicators of the geological source of rocks and artefacts. Mineral compositions have rarely been used in tectonic reconstructions and studies of archeological provenance. Examples of how minerals can be used for this type of study are provided by Le Bas (1962), Nisbet & Pearce (1977), and Leterrier

et al. (1982), who emphasized the utility of augite, and Maynard (1984), who focused on detrital plagioclase. In this study, we confirm the applicability of augite to studies of provenance in archeology and demonstrate that other minerals, in particular plagioclase and pigeonite, also are useful. In fact, we show that a combination of chemical information on plagioclase and augite provides discriminating capacity that may equal or rival whole-rock geochemistry. From an archeological perspective, the important aspect of these methods is that minuscule (1 mg) samples are required, and analyses are relatively inexpensive if a comparison database exists.

In this study, we use results of ~3700 electron-microprobe analyses of minerals to determine the bedrock source of 118 basalt "vessels" from ancient Egypt. These artefacts, found primarily in the graves of the elite members of society, are old, rare and valuable. Vessel manufacture began 800 years prior to the development of writing, peaked 200 years after the first known inscriptions, and continued for 400 years after Khufu built the great pyramid (Aston 1994, p. 85). The vessels examined here are from the earlier periods, the Predynastic (4000–3200 BCE) and Early Dynastic (Dynasty 0–1, 3200–2800 BCE; von der Way 1993, p. 83, 133), with the youngest predating the Great Pyramid by ~300 years. During this 1200-year period, when civilization first arose, about 600 vessels were manufactured (Mallory 2000, p. 22–87). They are important because they provide valuable information on trade patterns, social, and cultural practices during a time when there are few written records, or none at all.

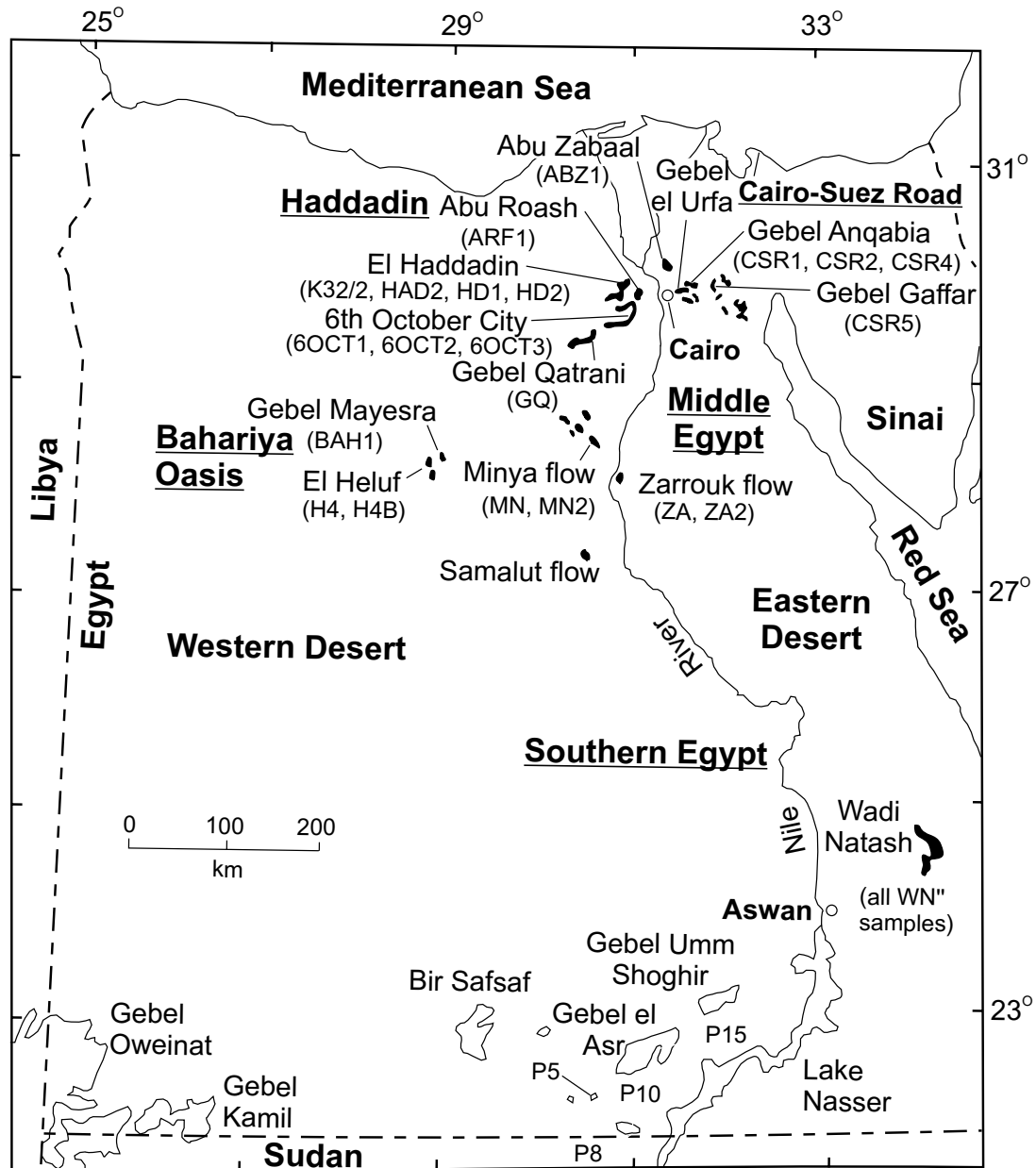


FIG. 1. Map of Egypt showing basalt flows (black) and areas containing igneous rocks (outlines). Samples are listed below locality names. Regions or flows are underlined. The Al-Fayoum region encompasses the Gebel Qatrani basalt outcrops and the area to the immediate south. Outcrop locations after Said (1962), Said & Martin (1964), El Hinnawi & Maksoud (1972), Awadallah (1980), Franz *et al.* (1987), Hubbard *et al.* (1987), and Meneisy (1990).

We present as an Appendix a selection of vessels that represent different sites, shapes and time periods. It was the damaged or fragmentary condition of these artefacts that permitted sampling. All were sampled for this project.

PREVIOUS PETROLOGICAL AND GEOCHEMICAL STUDIES ON THE VESSELS

The first scientific attempt to identify the geological source of the basalt used in Egyptian stone vessels is

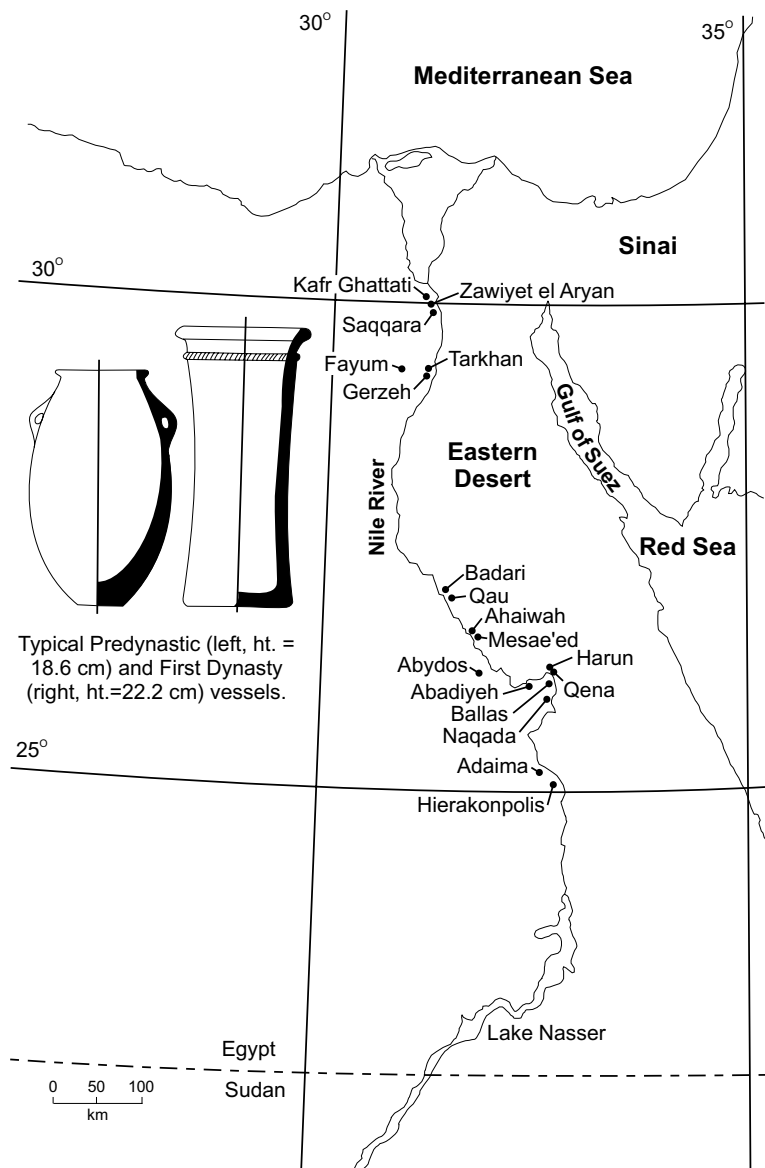


Fig. 2. Locations of archeological sites where the basalt vessels sampled for this study originated.

that of Lucas (1930). Using petrography, he concluded that the most likely source was Al-Fayoum, an area to the southwest of Cairo defined by the Gebel Qatrani basalt outcrops (Figs. 1, 2), as this was, in his opinion, where basalt paving stones were quarried during the Old Kingdom. Aston (1994) studied the various stones used to manufacture vessels from Predynastic to Roman times. She compared the petrography of basalt outcrops

to the west of Cairo (Fig. 1) and basalt vessels, but did not include other potential sources from east of Cairo, middle Egypt, or southern Egypt (Aston 1994, p. 18-21). The bedrock samples examined by Aston proved to be very uniform in mineralogy and texture, and, thus, she could not determine a specific flow or flows as the source for the basalt vessels (Aston 1994, p. 20). A recent survey of stone vessels from Abydos (Fig. 2)

contains petrographic descriptions of two basalt vessels, but the author did not attempt to establish their source (Schelstraete 1998, p. 47-48).

There are few published geochemical studies of Egyptian stone vessels. The most extensive to date is that of Schelstraete (1998), who surveyed the rock types used in the vessels found by Petrie during his excavations of the First Dynasty royal tombs at Abydos (Petrie 1900, 1901a, b, 1937). Although whole-rock X-ray fluorescence data were obtained for two basalt vessels (Schelstraete 1998, p. 72-74), no comparison between potential sources and the vessel data was made. In a more recent study, Greenough *et al.* (2001) compared whole-rock data from seven basalt vessels (excavated by Petrie at Abydos) to potential bedrock sources, and concluded that they were manufactured from the Haddadin basalt, which outcrops approximately 500 km north of Abydos and runs from Abu Zabaal (~50 km north of Cairo) to Al-Fayoum (~100 km southwest of Cairo; Figs. 1, 2). No other whole-rock data for basalt vessels have been published.

In a preliminary study, Mallory-Greenough *et al.* (1999) examined ten Predynastic (Naqada I and Naqada II) stone vessels from the collection of the Royal Ontario Museum (ROM1 to ROM10). Most of these vessels had been purchased from collectors, and information regarding their archeological origin may not be accurate. However, two of them were taken from the royal tombs at Abydos. All of the artefacts were intact, and it was not possible to use whole-rock analytical techniques to determine the source of the basalt. Instead, microsamples were removed from the bottom of the vessels or from damaged surfaces, and grain mounts were prepared. Augite and plagioclase in the vessels and potential bedrock sources were analyzed with an electron microprobe, and the data on minerals from the artefacts compared to those from the bedrock samples. One vessel (ROM 1) proved to be lamprophyric in composition, but the other nine (ROM2 to ROM10) were manufactured from basalt with chemical compositions of the constituent minerals matching those of the Haddadin basalt. This finding agrees with the whole-rock results, and suggests that on the basis of the composition of augite and plagioclase, the raw material or finished basalt vessels were transported from the Cairo area (Haddadin basalt flows) south to Qena and Abydos.

SAMPLING STRATEGY

Predynastic basalt vessels in the Royal Ontario Museum are made of fine-grained, undeformed and unaltered basalt (Mallory-Greenough *et al.* 1999). As the older volcanic rocks in Egypt tend to be regionally metamorphosed (Ressetar & Monrad 1983), the most likely sources of these fresh rocks are flows that are Late Cretaceous to Tertiary (Early Miocene) in age. Therefore, the rocks selected for comparison with the vessels are unaltered Tertiary subalkaline basalts from northern

(*e.g.*, Haddadin Basalt) and central Egypt, and Late Cretaceous alkaline basalts from southern Egypt (Fig. 1).

Our suite of bedrock samples represents all known unaltered flows or flow units in Egypt, regardless of whether or not they are considered to contain ancient quarries. All quarry sites compiled by Klemm & Klemm (1993) were sampled; their list is considered the most comprehensive survey. Although they were aware of the alkali basalts we sampled in southern Egypt, these rocks are not included in their work, nor were they considered potential sources by Lucas (1930), de Putter & Karlshausen (1992, p. 51-54), or Aston (1994, p. 19-20). Modern operations at quarries at Abu Zabaal and Tell el Haddadin (also called Tell el Zalut, at Abu Roash) may have destroyed evidence of earlier activity. Thus these sites could have been utilized in the past. The only confirmed ancient quarry is located at Al-Fayoum (Gebel Qatrani), but Old Kingdom workings have removed any traces of earlier Predynastic use (Harrell & Bown 1995). A comprehensive archeological survey of the other possible basalt sources, in which the potential ancient quarry sites are examined in detail, has not been conducted.

SAMPLE DESCRIPTIONS

Samples of bedrock basalt

Egyptian basalts can be divided into four petrological groups (Cairo, Bahariya, Middle Egypt, Southern Egypt) based on age, chemical composition, field relationships, and mineralogy. Further division on the basis of alkalinity (alkali basalt or tholeiite) yields five regions: subalkaline basalts are represented by Cairo–Suez Road, Haddadin, Bahariya, and Middle Egypt, and alkaline basalts by Southern Egypt. The Middle Egyptian samples (ZA, ZA2, MN, MN2) are probably from the same flow or flow sequence [paleomagnetic data: Wassif (1986), geochemistry: El Hinnawi & Maksoud (1972), Aly *et al.* (1983, p. 92)]. The Bahariya Oasis is represented by three samples, two from Gebel El Heluf or El Hufhuf (H4, H4B) and one from Gebel Mayesra (BAH1). Cairo-area basalts are divided into eastern and western flows based on age, paleomagnetism and petrology (Lotfy *et al.* 1995). The area west of Cairo contains the Haddadin basalt sequence, which runs from Abu Zabaal to the north of Cairo southward to Al-Fayoum and the western desert (Fig. 1). Multiple samples from various localities along the Haddadin flow were taken, including Abu Zabaal (ABZ1), Abu Roash (ARF1), Tell el Haddadin (HAD2, K32/2, HD1, HD2), Sixth of October City (6OCT1, 6OCT2, 6OCT3), and the ancient quarry at Gebel Qatrani (GQ). The Haddadin basalt sites approximately 10 km northeast of Maadi at Gebel Ahmar, Gebel el Saliman, and Gebel el Urfa were not sampled, as they are in a military area. Two sites to the east of Cairo (Cairo–Suez Road basalts) were

sampled, Gebel Anqabia (CSR1, CSR2, CSR4) and Gebel Gaffar (CSR5).

Alkali basalts were sampled in southern Egypt at Gebel el Asr, Lake Nasser, and Wadi Natash. Several basalt exposures occur as dikes near Gebel el Asr (Franz *et al.* 1987, Huth & Franz 1988). To the west of Lake Nasser are various basalt outcrops (P5, P8, P10; Franz *et al.* 1987) that are visible from the Aswan – Abu Simbel road. Three flow units, lower (WNL1, WNL5, WNL7), middle (WNL1, WNL2, WNL3) and upper (WNU2, WNU7, WNU8), and an eastern field (WN16) comprise the Wadi Natash basalts (Hubbard 1977, Crawford *et al.* 1984, Hubbard *et al.* 1987).

All samples of subalkaline basalt contain augite, plagioclase, pigeonite, olivine, and Fe–Ti oxides. Olivine is especially rare (< 1%) in the Haddadin and vessel samples. Pigeonite, though present, is not abundant in the northern samples. The alkaline southern basalts bear augite, plagioclase, Fe–Ti oxides, and olivine. Plagioclase in one Lake Nasser sample (P8) is altered. Matrix grain-sizes range from 0.1 mm (Cairo–Suez Road samples) to 0.6 mm (Abu Roash). Large (~1 cm) plagioclase phenocrysts are typical of the Haddadin basalts. Samples tend to be subophitic and microporphyritic (*i.e.*, contain augite, olivine or plagioclase micropenocrysts). Altered intersertal glass and olivine are present in the Abu Roash sample as green and brown (respectively) clay minerals.

Samples of basalt vessels

Vessels were selected for sampling on the basis of three criteria: published descriptions and photographs, provenance (archeological source of artefact is well documented), and accessibility (the likelihood that sampling would be permitted). For statistical purposes, an attempt was made to include as many different and widespread sites, vessel forms, and time periods as possible. Vessels of unusual form were included as well, even if their archeological context was not known. The important Predynastic sites of Abydos, Naqada, and Hierakonpolis (Fig. 2) were represented by multiple samples. Subsequently, vessels were eliminated from consideration either owing to their pristine condition (no surfaces suitable for sampling) or added if the vessel was not included in the original list, but met the criteria. As many of the museums visited do not have published catalogues, a number of artefacts were found after the initial list of samples had been created. The final set of samples contains one hundred and seventeen basalt vessels dating from the Badarian Period to the end of the First Dynasty, and covering sites from Kafr Ghattati north of Giza to Hierakonpolis in the south (Fig. 2). All major types of form or shape are represented by at least two samples, with the sample set representing 20% of the 598 Predynastic and First Dynasty basalt vessels known to exist (Mallory 2000, p. 22–87). Eight of the one hundred twenty-five vessels sampled, upon analy-

sis, proved to be manufactured from stones other than basalt (Mallory 2000, p. 167–169). Samples were obtained from the Ashmolean Museum, Oxford ('ASH' samples), British Museum, London (BM), Brooklyn Museum (BRK), Fitzwilliam Museum, Cambridge, U.K. (FIT), Museum of Fine Arts, Boston (MFA), Petrie Museum of Archaeology, London (PET), Royal Museums of Art and History, Brussels (RMB), and Royal Ontario Museum, Toronto (ROM).

ANALYTICAL AND SAMPLING METHODS

All 35 samples of bedrock were prepared as thick (0.3 mm) sections and analyzed for augite (total analyses ~500), plagioclase (~350), pigeonite (~35) and olivine (~112). For each sample, typically fifteen analyses of augite and plagioclase were made. We used the JEOL 733 electron microprobe at Dalhousie University. It is equipped with four wavelength-dispersion spectrometers and an Oxford Link eXL energy-dispersion system. The constituents SiO₂, TiO₂, Al₂O₃, Cr₂O₃, FeO, MnO, MgO, CaO, Na₂O, K₂O, La₂O₃, SrO, BaO, and NiO were detected using the energy-dispersion system with a resolution of 137 eV at 5.9 keV. The beam size was approximately 1 µm, with an accelerating voltage of 15 keV and a beam current of 15 nA. Spectrum acquisition lasted 40 seconds. All raw data were corrected by Oxford Link's ZAF matrix-correction program. Instrument calibration, performed on cobalt metal, was ±0.5% at one standard deviation. The mineral standards KK (amphibole) and KCpx (clinopyroxene) indicated a precision and an accuracy of better than ±2% for constituents with concentrations >1 wt.%. The typical detection-limit was ~0.1 wt.%. The trace elements La, Sr, Ba, and Ni are present at a level below detection except for Ni in olivine. All augite, pigeonite, plagioclase, and olivine compositions have analytical totals between 98.5 and 101.5 wt.%. Similarly, samples for which cation totals were greater than ±0.5% of the ideal total number were eliminated.

The value and importance of the vessels necessitated a microsampling technique. Thus a fine-tipped vibrating tool (vibrograver) was used to remove silt-sized to fine-grained sand-sized mineral particles from as many unfinished or broken surfaces on each vessel as possible. Each artefact sample (~1 mg) was prepared as thick (0.3 mm) grain mounts in epoxy, and augite (~1400 analyses), plagioclase (~1200), and, where possible, pigeonite (~90), and olivine (6 analyses), were analyzed using the Dalhousie microprobe (methods as above). Vessels ROM 1 to ROM 10 were analyzed at the University of Toronto using a Cameca SX50 electron microprobe, with three wavelength-dispersion spectrometers. Beam diameter (1 µm), operating conditions (15 keV and 30 nA), methods of calibration, and precision and accuracy are similar to those for the Dalhousie instrument. Average compositions of augite, plagioclase, pigeonite, and olivine in the bedrock samples and stone vessels appear

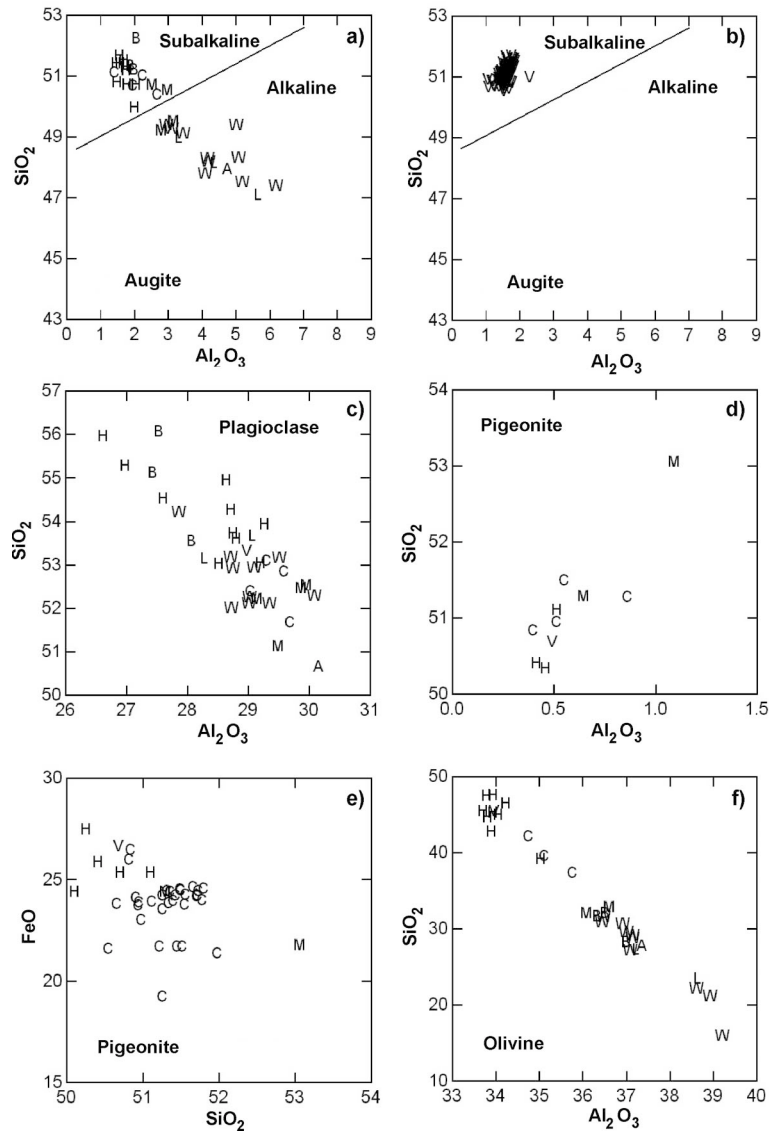


FIG. 3. Composition of augite from a) bedrock and b) vessel samples plotted on an Al_2O_3 versus SiO_2 (wt%) diagram. Fields after Le Bas (1962). Data used to create the diagram appear in Tables 1 and 3. Average Al_2O_3 versus SiO_2 (wt%) in plagioclase c) and pigeonite d) for bedrock samples (Table 1). All data (unaveraged) for pigeonite (e) plotted on a SiO_2 versus FeO diagram. Average compositions of olivine (f) on a SiO_2 versus FeO plot. For figures c, d, e, and f, the average of all vessels was used for clarity (Table 2). Symbols: A: Gebel el Asr, B: Bahariya, C: Cairo-Suez Road, H: Haddadin, L: Lake Nasser, M: Middle Egypt, V: Vessel(s), W: Wadi Natash.

in Tables 1, 2 and 3, respectively. Complete sets of mineral data are compiled as Appendices 2 (basalt bedrock), 3 (basalt vessels), and 4 (non-basalt vessels) in Mallory (2000), and are available from the first author.

DATA PRESENTATION

Differences in composition can be seen in the average data for augite, pigeonite, and plagioclase in each

TABLE 1. AVERAGE COMPOSITIONS OF MINERALS IN BEDROCK SAMPLES, EGYPTIAN BASALTS

Augite											Plagioclase								
Sample	N	SiO ₂	TiO ₂	Al ₂ O ₃	FeO	MnO	MgO	CaO	Na ₂ O	Total	Sample	N	SiO ₂	Al ₂ O ₃	FeO	CaO	Na ₂ O	K ₂ O	Total
Bahariya (T)											Bahariya								
H4	7	51.35	1.35	1.88	8.62	0.17	15.42	20.81	0.55	100.15	H4	2	53.56	28.01	0.60	11.30	4.62	0.30	98.39
H4B	14	51.24	1.19	1.99	8.11	0.07	15.66	20.35	0.43	99.04	H4B	12	55.14	27.44	0.64	9.70	5.58	0.39	98.89
BAH1	18	52.27	1.03	2.07	7.80	0.09	16.10	20.47	0.47	100.30	BAH1	15	56.08	27.53	0.70	9.75	5.61	0.42	100.09
Cairo-Suez Road (T)											Cairo-Suez Road								
CSR1	10	50.70	1.03	1.97	13.13	0.36	14.70	17.61	0.48	99.98	CSR1	6	52.41	29.04	0.91	12.51	4.25	0.20	99.32
CSR2	19	51.14	0.85	1.43	14.57	0.45	13.93	17.30	0.33	100.00	CSR2	22	52.86	29.59	0.90	12.61	4.20	0.23	100.39
CSR4	18	51.03	1.17	2.27	11.51	0.15	15.78	17.65	0.33	99.89	CSR4	19	53.10	29.31	0.83	12.13	4.30	0.27	99.94
CSR5	14	50.40	1.19	2.68	10.51	0.17	15.22	18.51	0.37	99.05	CSR5	19	51.69	29.69	0.89	12.81	3.87	0.18	99.13
Haddadin (T)											Haddadin								
ABZ1	22	51.21	1.01	1.78	11.34	0.24	15.53	18.22	0.32	99.65	ABZ1	20	53.06	29.22	0.79	11.85	4.45	0.29	99.66
ARF1	14	49.99	1.42	2.04	13.38	0.34	13.95	17.95	0.51	99.58	ARF1	5	55.29	26.99	0.59	10.21	5.23	0.34	98.65
K32/2	11	50.74	1.10	2.08	10.98	0.31	15.45	18.69	0.45	99.80	K32/2	3	54.55	27.62	0.73	10.74	5.04	0.36	99.04
HAD2	7	50.82	0.96	1.51	12.89	0.34	14.37	18.32	0.43	99.64	HAD2	4	55.97	26.63	0.89	9.55	5.57	0.41	99.02
HD1	11	51.54	1.13	1.72	12.36	0.31	15.09	17.96	0.34	100.45	HD1	9	53.73	28.77	0.85	11.65	4.66	0.32	99.98
HD2	9	51.69	1.02	1.60	12.32	0.31	15.23	17.83	0.28	100.28	HD2	9	54.28	28.73	0.75	11.50	4.72	0.30	100.28
6OCT1	9	51.45	1.03	1.50	13.94	0.36	14.28	17.56	0.34	100.46	6OCT1	8	54.95	28.66	0.81	11.19	5.02	0.36	100.99
6OCT2	9	51.31	1.18	1.76	12.64	0.31	14.59	18.18	0.34	100.31	6OCT2	10	53.95	29.28	0.87	11.91	4.71	0.30	101.02
6OCT3	13	51.43	1.07	1.61	11.61	0.26	15.01	18.56	0.34	99.89	6OCT3	14	53.62	28.82	0.80	11.82	4.67	0.27	100.00
GQ	25	50.75	1.00	1.80	12.96	0.21	14.88	17.97	0.30	99.87	GQ	13	53.04	28.53	0.90	11.62	4.77	0.34	99.20
Middle Egypt (T)											Middle Egypt								
ZA	9	49.23	1.85	2.80	13.07	0.33	14.42	17.40	0.44	99.54	ZA	4	51.14	29.50	0.98	13.49	3.78	0.10	98.99
ZA2	14	50.57	1.41	2.99	11.99	0.20	14.45	18.47	0.40	100.48	ZA2	17	52.54	29.96	0.83	13.08	3.96	0.13	100.50
MN	9	49.55	1.41	3.18	10.62	0.21	15.25	18.64	0.49	99.35	MN	2	52.22	29.15	0.77	12.68	4.08	0.16	99.06
MN2	19	50.73	1.33	2.52	12.79	0.33	15.14	17.05	0.35	100.24	MN2	22	52.48	29.87	0.86	13.05	4.04	0.15	100.45
Wadi Natash (A)											Wadi Natash								
WN16	17	49.29	1.88	3.12	10.18	0.13	14.59	20.10	0.49	99.78	WN16	9	54.23	27.88	0.96	10.52	5.32	0.45	99.36
WNL1	10	48.35	2.49	5.12	8.48	0.16	13.49	21.69	0.58	100.36	WNL1	8	53.18	29.52	0.94	11.98	4.49	0.28	100.50
WNL5	12	49.13	2.27	3.47	9.07	0.07	13.92	21.51	0.60	100.04	WNL5	10	53.19	28.73	0.80	11.46	4.90	0.29	99.37
WNL7	9	49.42	1.80	2.97	10.02	0.17	13.64	21.05	0.59	99.66	WNL7	8	52.94	28.76	0.75	11.45	4.77	0.32	98.99
WNM1	8	47.53	2.46	5.22	8.14	b.d.	13.14	22.03	0.63	99.15	WNM1	5	52.02	28.73	1.04	11.46	4.46	0.42	98.13
WNM2	10	49.41	1.93	5.04	7.62	0.10	13.73	21.89	0.66	100.11	WNM2	10	52.30	30.10	0.64	12.68	4.18	0.24	100.14
WNM3	12	47.80	2.49	4.12	9.32	0.07	13.14	21.59	0.66	99.19	WNM3	5	52.12	29.02	0.80	11.82	4.55	0.31	98.62
WNU2	10	47.43	1.97	6.23	6.80	b.d.	13.67	21.62	0.67	98.50	WNU2	5	52.26	29.03	0.81	11.56	4.61	0.35	98.62
WNU7	14	48.20	2.38	4.20	9.13	b.d.	13.38	21.66	0.58	99.53	WNU7	10	52.13	29.36	0.80	12.17	4.46	0.26	99.18
WNU8	5	48.30	2.60	4.18	9.20	0.13	13.13	21.56	0.78	99.88	WNU8	5	52.94	29.12	0.89	11.54	4.80	0.32	99.61
Gebel el Asr (A)											Gebel el Asr								
P15	16	47.95	2.38	4.76	8.81	0.06	13.65	21.20	0.58	99.39	P15	10	50.68	30.16	0.78	13.19	3.81	0.34	98.96
Lake Nasser (A)											Lake Nasser								
P5	14	47.10	3.45	5.65	8.64	0.06	12.82	21.57	0.68	99.97	P5	12	53.68	29.08	0.97	11.49	4.65	0.47	100.34
P8	15	48.16	2.60	4.35	9.23	0.07	13.03	21.88	0.64	99.96	P8	no unaltered plagioclase present							
P10	15	48.98	2.00	3.31	8.75	b.d.	13.83	21.79	0.60	99.26	P10	6	53.16	28.28	0.88	11.03	5.07	0.34	98.76
Pigeonite																			
Cairo-Suez Road																			
CSR1	6	50.96	0.52	0.52	24.21	0.78	17.67	4.59	0.32	99.57									
CSR2	17	51.51	0.46	0.55	24.26	0.73	17.47	4.72	0.12	99.82									
CSR4	1	50.84	0.50	0.40	26.51	0.75	15.73	4.96	b.d.	99.69									
CSR5	7	51.28	0.61	0.86	21.50	0.60	18.79	5.40	b.d.	99.04									
Haddadin																			
ABZ1	2	50.34	0.55	0.46	26.70	0.76	15.47	4.84	b.d.	99.12									
HAD2	2	50.42	0.43	0.42	25.91	0.67	15.39	4.99	0.34	98.57									
6OCT3	1	51.12	0.59	0.52	25.38	0.62	14.70	6.84	b.d.	99.77									
Middle Egypt																			
ZA2	1	53.07	0.67	1.09	21.80	0.66	19.53	4.45	b.d.	101.27									
MN	1	51.29	0.51	0.65	24.44	0.52	17.74	4.65	0.32	100.12									

Olivine								Olivine							
Sample	N	SiO ₂	FeO	MnO	MgO	CaO	Total	Sample	N	SiO ₂	FeO	MnO	MgO	CaO	Total
Bahariya								Middle Egypt							
H4	6	37.01	28.34	0.36	34.26	0.32	100.29	MN	6	36.09	32.11	0.48	30.89	0.26	99.83
H4B	3	36.33	31.74	0.29	31.41	0.32	100.09	MN2	7	36.62	32.98	0.50	30.54	0.25	100.89
BAH1	6	36.52	32.15	0.43	30.75	0.29	100.14	Wadi Natash							
Cairo-Suez Road								WN16	6	37.17	27.82	0.47	35.35	0.27	101.08
CSR1	4	35.13	39.69	0.68	25.02	0.24	100.76	WNL1	6	38.96	21.26	0.37	40.21	0.30	101.10
CSR2	3	35.78	37.40	0.70	26.63	0.26	100.77	WNL5	2	36.95	29.78	0.43	34.22	0.38	101.76
CSR4	3	34.77	42.30	0.67	22.93	0.37	101.04	WNL7	1	36.46	29.96	0.50	33.73	0.36	101.01
Haddadin								WNM1	1	37.12	27.20	0.44	36.14	0.36	101.26
ABZ1	2	33.73	45.58	0.68	19.37	0.27	99.63	WNM2	4	38.64	22.25	0.32	39.59	0.30	101.10
K32/2	7	33.91	42.88	0.70	21.38	0.28	99.15	WNM3	2	36.51	31.61	0.49	32.64	0.39	101.64
HAD2	3	33.83	44.77	0.81	19.91	0.23	99.55	WNU2	3	39.23	16.08	0.10	45.56	0.18	101.15
HD1	2	34.07	45.04	0.61	19.98	0.22	99.92	WNU7	2	37.03	29.67	0.46	34.36	0.26	101.78
HD2	2	33.96	47.70	0.74	18.43	0.23	101.06	WNU8	2	36.76	28.74	0.67	34.81	0.23	101.21
6OCT1	2	35.06	39.27	0.60	24.94	0.28	100.15	Gebel el Asr							
6OCT2	2	34.25	46.59	0.81	19.47	0.25	101.37	P15	4	37.38	27.80	0.42	35.81	0.31	101.72
6OCT3	2	33.95	45.40	0.74	19.33	0.30	99.72	Lake Nasser							
GQ	6	33.82	46.52	0.68	20.00	0.22	101.24	P5	4	38.65	23.50	0.46	38.67	0.36	101.64
								P8	4	36.59	32.52	0.39	32.67	0.31	101.48
								P10	5	37.23	27.37	0.40	36.15	0.30	101.45

Raw data, calculation procedures, and standard deviations are given in Appendix 2, Mallory (2000). Compositions are reported as wt.% oxides. N: number of analyses. b.d.: below detection limit. A: alkali basalt, T: tholeiite.

TABLE 2. AVERAGE COMPOSITIONS OF MINERALS IN ALL BASALT VESSELS

Mineral		N	SiO ₂	TiO ₂	Al ₂ O ₃	FeO	MnO	MgO	CaO	Na ₂ O	K ₂ O
Augite	average	117	51.14	1.01	1.61	12.54	0.26	14.95	17.91	0.31	
	st. dev.		0.26	0.07	0.16	1.44	0.07	0.55	0.66	0.05	
Plagioclase	average	117	53.33		28.99	0.77			11.65	4.60	§0.29
	st. dev.		0.65		0.48	0.07			0.50	0.31	0.37
Pigeonite	average	53	50.69	0.45	0.49	26.68	0.69	15.50	5.07	0.08	
	st. dev.		0.43	0.13	0.15	1.55	0.08	1.03	0.97	0.07	
Olivine	average	7	33.98			45.52	0.76	19.84	0.27		
	st. dev.		0.43			1.56	0.10	1.32	0.07		

N: number of vessels, st. dev.: standard deviation. § The concentration of potassium was not measured in plagioclase for samples ROM2 to ROM10. It was thus measured in 108 vessels rather than 117.

bedrock sample (Table 1) and, in particular, among bedrock units. For example, the average amount of Mn in the Bahariyan augite (0.07–0.17 wt.% MnO) is lower than in Haddadin augite (0.24–0.36 wt.% MnO).

Figure 3a shows that average compositions of augite in the bedrock, plotted as Al₂O₃ versus SiO₂, encompass a wide range of compositions that cross both the alkaline and tholeiitic fields (Le Bas 1962). Average SiO₂ and Al₂O₃ values for augite in the 117 vessels (summary of ~1400 analyses; averages in Table 3) en-

compass a very small range of subalkaline compositions (Fig. 3b) that overlap with augite from Haddadin, Cairo-Suez and Middle Egypt suites (Fig. 3a). As it is difficult to see relationships and similarities when hundreds of data points are plotted on a diagram, averages (Tables 1, 2) have been used for clarity in Figure 3c, d, e, and f. As in augite, SiO₂ and Al₂O₃ are negatively correlated in plagioclase (Fig. 3c), but there is no obvious correlation in pigeonite (Fig. 3d). Perhaps this reflects the small range of compositions shown by northern subalkaline

TABLE 3. AVERAGE MINERAL COMPOSITIONS FOR INDIVIDUAL BASALT VESSEL SAMPLES

Augite																					
Sample	N	SiO ₂	TiO ₂	Al ₂ O ₃	FeO	MnO	MgO	CaO	Na ₂ O	Total	Sample	N	SiO ₂	TiO ₂	Al ₂ O ₃	FeO	MnO	MgO	CaO	Na ₂ O	Total
ASH1	13	51.06	0.96	1.48	13.12	0.30	14.55	17.75	0.34	99.56	PET15	15	50.99	0.97	1.41	13.83	0.29	14.54	17.21	0.35	99.59
ASH2	10	51.11	1.11	1.74	11.49	0.28	15.26	18.34	0.34	99.67	PET16	17	51.07	1.06	1.66	12.30	0.20	15.04	18.05	0.34	99.72
ASH3	1	51.18	1.03	1.45	13.61	0.36	14.55	17.43	0.42	100.03	PET17	12	51.00	0.99	1.59	13.41	0.30	14.53	17.42	0.23	99.47
ASH4	3	50.88	0.71	1.24	16.34	0.43	13.74	16.02	0.40	99.96	PET18	12	51.45	1.01	1.59	11.88	0.25	15.26	18.30	0.34	100.08
ASH5	10	51.14	1.01	1.65	12.18	0.42	15.01	17.97	0.33	99.71	RMB1	8	51.48	0.98	1.53	12.46	0.24	15.02	18.12	0.29	100.12
ASH6	15	50.92	0.98	1.44	14.38	0.29	14.28	16.99	0.32	99.60	RMB2	6	51.29	1.07	1.67	11.60	0.23	15.25	18.48	0.33	99.92
ASH7	11	51.46	0.99	1.73	10.90	0.21	15.45	18.77	0.29	99.80	RMB4	14	51.36	1.00	1.63	11.52	0.22	15.30	18.44	0.28	99.75
ASH8	9	51.18	0.98	1.51	12.44	0.30	14.99	18.03	0.34	99.77	RMB5	3	50.72	0.91	1.29	15.24	0.43	14.00	16.49	0.39	99.47
ASH9	10	50.89	1.10	1.59	12.25	0.19	14.97	17.97	0.20	99.16	RMB6	9	51.59	1.09	1.65	12.37	0.20	15.22	18.10	0.33	100.55
ASH10	18	51.28	1.03	1.57	12.27	0.26	15.04	18.04	0.33	99.82	RMB7	10	51.33	0.96	1.58	11.57	0.28	15.28	18.33	0.31	99.64
ASH11	10	50.75	1.08	1.56	13.25	0.28	14.40	17.76	0.31	99.39	RMB8	12	51.29	1.06	1.58	11.86	0.22	15.15	18.26	0.27	99.69
ASH12	16	51.07	1.05	1.56	12.87	0.25	14.72	17.86	0.34	99.72	RMB9	12	51.34	1.03	1.63	11.81	0.21	15.22	18.40	0.31	99.95
ASH13	10	51.04	0.95	1.48	13.93	0.30	14.83	17.04	0.33	99.90	RMB10	9	50.73	0.91	1.42	16.87	0.46	13.16	16.28	0.29	100.12
BM1	10	51.24	1.01	1.69	11.87	0.28	15.23	18.22	0.29	99.83	RMB11	10	50.99	0.94	1.40	13.42	0.28	14.53	17.67	0.34	99.57
BM2	7	50.90	0.95	1.19	15.32	0.37	13.65	16.13	0.35	98.86	RMB12	12	51.02	1.10	1.63	12.30	0.14	15.13	17.91	0.28	99.51
BM3	11	51.55	0.94	1.88	9.57	0.12	16.31	18.57	0.25	99.19	RMB13	11	51.17	0.94	1.43	14.93	0.28	14.71	17.24	0.27	100.97
BM4	11	51.23	1.04	1.76	11.30	0.23	15.25	18.54	0.34	99.69	RMB14	22	51.12	1.03	1.62	12.81	0.24	15.01	17.66	0.35	99.84
BM5	12	50.75	1.09	1.63	12.48	0.36	14.68	17.78	0.30	99.07	RMB15	15	50.85	1.11	1.57	13.44	0.32	14.60	17.58	0.38	99.85
BRK1	11	51.35	1.11	1.87	10.64	0.11	15.76	18.43	0.34	99.61	RMB16	12	51.19	1.08	1.74	11.21	0.20	15.48	18.48	0.29	99.67
BRK2	13	51.09	1.09	1.68	12.41	0.25	15.07	17.95	0.33	99.87	RMB17	17	51.40	1.08	1.69	10.62	0.19	15.64	18.68	0.31	99.61
BRK3	10	51.26	1.03	1.67	11.91	0.24	15.27	18.30	0.32	100.00	RMB18	6	50.80	1.03	1.55	14.21	0.39	14.31	17.21	0.24	99.74
BRK4	12	50.96	1.06	1.66	13.11	0.30	14.37	17.89	0.33	99.68	RMB19	16	51.34	1.03	1.63	12.06	0.24	15.15	18.23	0.30	99.98
BRK5	8	50.76	0.85	1.25	15.58	0.40	13.65	16.65	0.36	99.50	RMB20	12	50.89	1.05	1.61	12.70	0.30	14.80	17.91	0.36	99.62
BRK6	16	51.23	1.04	1.61	12.03	0.26	15.16	18.17	0.35	99.85	RMB21	18	51.48	1.10	1.67	10.86	0.23	15.67	18.69	0.30	100.00
BRK7	11	51.35	1.04	1.65	11.81	0.23	15.28	18.30	0.34	100.00	RMB22	12	51.30	1.06	1.80	11.28	0.17	15.39	18.49	0.33	99.82
BRK8	19	51.40	1.06	1.80	11.11	0.20	15.67	18.29	0.31	99.84	RMB23	18	51.26	1.01	1.57	12.04	0.23	15.28	17.97	0.35	99.71
FIT1	10	50.94	1.00	1.49	13.45	0.27	14.30	17.70	0.29	99.44	RMB24	18	51.21	1.01	1.63	12.49	0.25	14.93	18.07	0.32	99.91
FIT2	16	51.23	1.06	1.63	12.16	0.25	15.01	18.24	0.34	99.92	RMB25	11	50.78	0.94	1.48	13.51	0.33	14.71	17.24	0.34	99.33
FIT3	12	51.01	1.02	2.31	10.30	0.14	15.79	18.44	0.30	99.31	RMB26	11	50.91	0.93	1.37	14.72	0.36	14.07	17.24	0.35	99.95
FIT4	9	51.10	1.05	1.68	12.44	0.18	14.88	17.98	0.33	99.64	RMB28	12	50.92	0.96	1.50	13.43	0.38	14.45	17.61	0.31	99.56
MFA1	11	51.42	1.03	1.76	10.37	0.16	15.60	18.97	0.35	99.66	RMB29	11	51.57	0.93	1.82	9.35	0.16	16.24	19.05	0.26	99.38
MFA2	8	50.93	0.97	1.39	13.13	0.25	14.68	17.49	0.23	99.07	RMB30	11	50.93	1.09	1.66	12.04	0.20	15.05	18.06	0.34	99.37
MFA3	15	51.31	0.97	1.61	12.59	0.26	14.88	18.00	0.31	99.93	RMB31	3	50.56	0.99	1.56	13.08	0.19	14.66	17.62	0.23	98.89
MFA4	14	50.87	0.98	1.76	12.92	0.26	14.81	17.57	0.36	99.53	RMB32	11	50.63	0.98	1.57	12.89	0.33	14.65	17.67	0.35	99.07
MFA5	17	51.14	1.07	1.61	12.20	0.24	15.07	18.00	0.24	99.57	RMB33	6	50.64	1.08	1.71	11.92	0.27	14.93	18.07	0.33	98.95
MFA6	23	51.22	1.02	1.66	11.61	0.17	15.21	18.45	0.32	99.66	RMB34	12	50.83	1.03	1.58	12.47	0.33	14.90	17.75	0.28	99.17
MFA7	12	50.97	1.14	1.68	11.14	0.18	15.39	18.49	0.28	99.27	RMB35	10	50.64	1.00	1.56	13.04	0.27	14.61	17.37	0.35	98.84
MFA8	11	50.89	1.05	1.65	12.90	0.26	14.77	17.60	0.32	99.44	RMB36	10	51.11	1.02	1.47	12.79	0.19	14.72	17.95	0.37	99.62
MFA9	18	50.96	0.95	1.58	13.69	0.31	14.46	17.41	0.33	99.69	RMB37	12	51.11	1.00	1.40	14.47	0.35	14.51	17.01	0.32	100.17
MFA10	12	51.03	0.96	1.52	12.48	0.28	14.91	17.99	0.32	99.49	RMB39	11	51.65	1.01	1.81	10.69	0.19	15.80	18.72	0.32	100.19
MFA12	15	50.99	0.97	1.47	13.71	0.28	14.62	17.29	0.31	99.64	RMB40	6	51.13	0.97	1.48	14.36	0.38	14.81	16.89	0.31	99.33
MFA13	17	51.17	1.00	1.64	12.14	0.31	15.23	17.96	0.30	99.75	ROM2	16	51.27	0.99	1.68	12.75	0.32	14.71	18.18	0.23	100.13
MFA14	17	51.19	1.04	1.68	11.94	0.24	15.36	17.98	0.32	99.75	ROM3	4	51.35	1.06	1.73	11.94	0.31	15.16	18.15	0.22	99.92
MFA15	15	51.04	1.04	1.61	12.22	0.23	14.97	18.19	0.32	99.62	ROM4	9	51.62	0.99	1.82	10.69	0.26	15.62	19.08	0.23	100.31
MFA16	10	51.23	0.99	1.68	11.81	0.22	15.24	18.19	0.33	99.69	ROM5	7	51.63	0.98	1.66	11.77	0.32	15.19	18.49	0.22	100.26
MFA17	9	50.87	1.08	1.48	13.89	0.28	14.36	17.25	0.34	99.55	ROM6	14	51.26	0.98	1.75	12.22	0.32	14.93	18.36	0.23	100.05
MFA18	13	51.09	1.09	1.67	12.05	0.22	15.10	17.96	0.32	99.50	ROM7	11	51.30	1.02	1.71	12.73	0.33	14.87	18.17	0.24	100.37
MFA19	16	51.24	0.97	1.60	12.76	0.24	15.21	17.37	0.30	99.69	ROM8	11	51.23	0.93	1.49	15.11	0.40	14.00	16.87	0.24	100.27
PET1	8	51.00	1.15	1.73	11.56	0.09	15.00	18.36	0.32	99.21	ROM9	10	51.42	1.05	1.79	12.09	0.31	14.87	18.55	0.22	100.30
PET2	6	50.93	0.79	1.07	17.64	0.43	13.92	14.94	0.09	99.81	ROM10	17	51.34	1.00	1.74	13.04	0.33	14.71	17.99	0.23	100.38
PET3	17	51.17	0.98	1.55	12.91	0.28	14.66	17.91	0.29	99.75	ROM11	11	51.10	1.09	1.76	10.42	0.25	15.42	18.95	0.40	99.39
PET5	4	50.68	0.83	1.10	16.49	0.43	13.19	16.47	0.28	99.47	ROM12	10	51.61	0.93	1.87	11.42	0.18	15.65	18.17	0.31	100.14
PET7	16	50.84	1.00	1.50	13.34	0.26	14.54	17.53	0.35	99.36	ROM13	10	51.41	1.04	1.62	12.64	0.26	14.99	18.08	0.34	100.38
PET8	10	51.17	1.02	1.58	12.35	0.24	15.02	17.99	0.30	99.67	ROM15	12	51.42	1.09	1.64	11.56	0.20	15.48	18.33	0.34	100.06
PET9	15	51.24	0.98	1.71	11.40	0.19	15.32	18.42	0.36	99.62	ROM16	11	51.69	0.93	1.63	11.79	0.23	15.42	18.27	0.31	100.27
PET11	17	51.13	1.10	1.68	12.10	0.23	15.14	18.10	0.31	99.79	ROM17	9	51.59	0.95	1.66	10.76	0.26	15.72	18.74	0.27	99.95
PET12	8	50.83	0.99	1.80	11.42	0.26	15.25	18.06	0.26	98.87	ROM18	11	51.34	1.04	1.67	12.90	0.30	15.08	18.37	0.32	100.12
PET13	15	51.70	0.89	1.77	11.01	0.21	16.01	18.03	0.22	99.84	ROM19	12	51.20	1.16	1.68	12.00	0.28	14.69	18.03	0.30	100.24
PET14																					

TABLE 3 (continued). AVERAGE MINERAL COMPOSITIONS FOR INDIVIDUAL BASALT VESSEL SAMPLES

Plagioclase																	
Sample	N	SiO ₂	Al ₂ O ₃	FeO	CaO	Na ₂ O	K ₂ O	Total	Sample	N	SiO ₂	Al ₂ O ₃	FeO	CaO	Na ₂ O	K ₂ O	Total
ASH1	8	53.61	28.97	0.75	11.48	4.77	0.30	99.88	PET14	17	53.26	29.10	0.74	11.73	4.56	0.27	99.66
ASH2	5	52.59	29.46	0.60	12.32	4.33	0.20	99.50	PET15	11	52.98	29.45	0.77	12.01	4.46	0.25	99.92
ASH3	11	55.87	27.01	0.65	9.80	5.81	0.43	99.57	PET16	12	52.61	29.46	0.78	12.16	4.29	0.24	99.54
ASH4	7	54.62	27.66	0.53	11.37	5.32	0.34	99.84	PET17	7	52.62	29.24	0.76	12.00	4.34	0.25	99.21
ASH5	7	52.90	29.05	0.61	11.90	4.49	0.28	99.23	PET18	12	52.97	29.48	0.77	12.05	4.31	0.25	99.83
ASH6	9	54.30	28.53	0.87	10.98	4.85	0.31	99.84	RMB1	8	54.08	28.85	0.96	11.35	4.95	0.32	100.51
ASH7	10	52.95	29.40	0.77	11.99	4.51	0.24	99.86	RMB2	9	52.77	29.21	0.99	12.23	4.36	0.25	99.81
ASH8	7	51.79	29.80	0.80	12.62	4.08	0.23	99.32	RMB4	11	53.41	28.84	0.78	11.39	4.75	0.31	99.48
ASH9	13	52.76	28.23	0.76	11.82	4.52	0.26	98.35	RMB5	6	52.97	28.99	1.04	11.70	4.58	0.27	99.55
ASH10	12	53.45	28.96	0.74	11.55	4.73	0.28	99.71	RMB6	11	53.19	29.32	0.76	12.01	4.54	0.25	100.07
ASH11	8	52.72	29.10	0.85	11.97	4.45	0.25	99.34	RMB7	8	53.24	28.74	0.74	11.50	4.60	0.29	99.11
ASH12	13	53.59	28.91	0.70	11.43	4.77	0.30	99.70	RMB8	8	54.05	28.53	0.82	11.03	4.92	0.32	99.67
ASH13	5	54.01	28.41	0.81	10.98	4.89	0.31	99.41	RMB9	12	53.25	28.96	0.85	11.60	4.67	0.30	99.63
BM1	10	53.79	28.84	0.71	11.35	4.81	0.31	99.81	RMB10	10	54.35	28.46	0.82	10.93	5.06	0.37	99.99
BM2	10	52.93	29.31	0.78	11.88	4.49	0.27	99.66	RMB11	4	53.78	28.88	0.80	11.39	4.73	0.28	99.86
BM3	9	52.63	29.18	0.72	12.00	4.40	0.26	99.19	RMB12	10	53.08	29.02	0.75	11.80	4.60	0.29	99.54
BM4	8	54.13	28.62	0.75	11.13	4.97	0.31	99.91	RMB13	15	53.44	29.20	0.74	11.73	4.67	0.29	100.07
BM5	10	52.66	28.90	0.73	11.79	4.52	0.27	98.87	RMB14	19	53.78	28.81	0.78	11.41	4.78	0.30	99.86
BRK1	14	52.81	29.39	0.77	12.08	4.39	0.25	99.69	RMB15	17	53.75	28.66	0.78	11.31	4.84	0.31	99.65
BRK2	13	53.45	28.88	0.83	11.53	4.71	0.32	99.72	RMB16	11	53.17	29.02	0.81	11.69	4.67	0.26	99.62
BRK3	10	52.14	29.87	0.81	12.51	4.18	0.24	99.75	RMB17	17	53.03	29.20	0.79	11.88	4.52	0.26	99.50
BRK4	10	52.98	29.27	0.77	11.97	4.44	0.25	99.68	RMB18	8	53.05	29.28	0.77	11.95	4.52	0.25	99.82
BRK5	7	52.94	29.09	0.75	11.74	4.54	0.29	99.35	RMB19	16	53.90	28.78	0.77	11.30	4.88	0.31	99.94
BRK6	14	53.84	28.78	0.90	11.37	4.82	0.30	100.01	RMB20	11	52.81	29.23	0.81	11.88	4.51	0.27	99.51
BRK7	9	54.95	28.15	0.71	10.43	5.28	0.37	99.89	RMB21	18	53.15	29.28	0.75	11.88	4.56	0.27	99.89
BRK8	17	53.11	29.17	0.82	11.75	4.54	0.30	99.69	RMB22	12	53.28	29.13	0.76	11.75	4.56	0.28	99.76
FIT1	10	53.50	29.12	0.81	11.62	4.66	0.28	99.99	RMB23	17	52.65	29.31	0.74	12.03	4.42	0.26	99.41
FIT2	14	53.35	29.04	0.70	11.60	4.56	0.29	99.54	RMB24	16	52.83	29.35	0.77	12.03	4.44	0.26	99.68
FIT3	9	52.54	29.59	0.65	12.33	4.29	0.22	99.62	RMB25	8	52.69	29.24	0.77	11.84	4.43	0.24	99.21
FIT4	10	54.69	28.12	0.77	10.59	5.23	0.36	99.76	RMB26	10	53.92	28.71	0.74	11.21	4.88	0.30	99.76
MFA1	15	53.95	28.53	0.74	11.07	4.94	0.31	99.54	RMB28	9	53.77	28.43	0.77	11.04	4.87	0.32	99.20
MFA2	10	53.59	28.48	0.74	11.20	4.80	0.32	99.13	RMB29	10	53.00	29.14	0.81	11.71	4.50	0.29	99.45
MFA3	11	55.46	27.77	0.77	10.11	5.50	0.43	100.04	RMB30	12	53.37	28.63	0.76	11.31	4.81	0.32	99.20
MFA4	11	53.06	29.16	0.72	11.74	4.51	0.26	99.45	RMB31	5	53.46	28.63	0.78	11.23	4.79	0.29	99.18
MFA5	18	53.75	28.47	0.79	11.03	4.92	0.33	99.29	RMB32	10	53.36	28.41	0.85	11.26	4.78	0.28	98.94
MFA6	25	54.01	28.56	0.81	10.99	4.95	0.33	99.65	RMB33	9	53.63	27.97	0.79	10.94	4.88	0.33	98.54
MFA7	10	53.60	28.48	0.86	11.09	4.85	0.32	99.20	RMB34	9	53.48	28.49	0.81	11.19	4.85	0.31	99.13
MFA8	14	52.92	29.15	0.79	11.86	4.52	0.27	99.51	RMB35	10	52.78	28.94	0.74	11.72	4.52	0.26	98.96
MFA9	17	53.42	28.84	0.77	11.48	4.68	0.31	99.50	RMB36	9	53.35	28.98	0.77	11.60	4.70	0.26	99.66
MFA10	13	54.04	28.30	0.77	10.86	5.02	0.32	99.31	RMB37	10	53.02	29.35	0.73	11.95	4.47	0.27	99.79
MFA12	13	54.24	28.25	0.75	10.89	5.04	0.34	99.51	RMB39	10	52.56	29.63	0.76	12.31	4.29	0.25	99.80
MFA13	17	52.64	29.31	0.82	12.06	4.37	0.25	99.45	RMB40	9	53.39	29.11	0.73	11.80	4.64	0.28	99.95
MFA14	17	52.85	29.30	0.75	11.91	4.42	0.27	99.50	ROM2	15	53.94	28.99	0.75	11.68	4.24	N.A.	99.60
MFA15	16	53.05	28.98	0.86	11.78	4.53	0.26	99.46	ROM3	1	53.04	30.19	0.70	12.69	3.85	N.A.	100.47
MFA16	10	54.30	28.28	0.78	10.81	5.04	0.36	99.57	ROM4	12	54.46	28.68	0.73	11.24	4.46	N.A.	99.57
MFA17	12	53.28	28.73	0.84	11.48	4.63	0.29	99.25	ROM5	8	53.54	29.24	1.05	12.01	4.03	N.A.	99.87
MFA18	12	52.98	29.12	0.69	11.81	4.54	0.26	99.40	ROM6	9	53.34	29.56	0.73	12.22	4.01	N.A.	99.86
MFA19	16	52.53	29.43	0.77	12.18	4.33	0.25	99.49	ROM7	9	53.49	29.70	0.79	12.26	4.11	N.A.	100.35
PET1	10	52.47	29.34	0.77	12.17	4.30	0.26	99.31	ROM8	9	54.00	29.30	0.72	11.99	4.11	N.A.	100.12
PET2	9	52.84	29.15	0.67	11.90	4.43	0.25	99.24	ROM9	8	53.49	29.60	0.73	12.25	4.03	N.A.	100.10
PET3	12	52.97	29.19	0.77	11.85	4.54	0.28	99.60	ROM10	12	54.17	29.12	0.81	11.62	4.35	N.A.	100.07
PET5	4	53.50	28.65	0.70	11.21	4.78	0.32	99.16	ROM11	10	53.05	28.81	0.76	11.50	4.67	0.27	99.06
PET7	14	52.89	29.10	0.73	11.80	4.53	0.29	99.34	ROM12	10	52.70	29.80	0.70	12.44	4.23	0.22	100.09
PET8	6	52.96	28.90	0.84	11.59	4.51	0.30	99.10	ROM13	9	53.34	29.31	0.78	11.88	4.55	0.29	100.15
PET9	13	52.69	29.19	0.86	11.95	4.44	0.24	99.37	ROM15	9	53.40	29.25	0.72	11.83	4.60	0.26	100.06
PET11	15	52.59	29.43	0.83	12.12	4.36	0.25	99.58	ROM16	8	52.75	29.97	0.77	12.50	4.28	0.22	100.49
PET12	13	52.73	28.91	0.79	11.66	4.51	0.28	98.88	ROM17	8	53.99	29.00	0.73	11.42	4.77	0.30	100.21
PET13	16	52.51	29.67	0.81	12.30	4.28	0.25	99.82	ROM18	5	52.79	29.61	0.79	12.30	4.41	0.24	100.14
									ROM19	9	53.85	28.82	0.74	11.27	4.89	0.30	99.87

ratios derived from Tables 1 and 2). In Figure 4b, weight-percent plots of the anorthite component of plagioclase and the wollastonite component of augite illustrate that $\text{CaO}/(\text{CaO} + \text{MgO} + \text{FeO})$ in augite is lower in Haddadin, Cairo–Suez and Middle Egypt flows than in Bahariya and southern Egypt (Wadi Natash, Lake Nasser Gebel et Asr), and that $\text{CaO}/(\text{CaO} + \text{Na}_2\text{O} +$

$\text{K}_2\text{O})$ in plagioclase is lower in Haddadin samples than in Cairo–Suez and Middle Egypt samples. Thus, most major groups of rocks are separated on this diagram; the average of all vessels plots with the Haddadin averages. Ratios of some trace components in augite (MnO/TiO_2 ; $\text{SiO}_2/\text{TiO}_2$) and plagioclase ($\text{K}_2\text{O}/\text{FeO}$; $\text{K}_2\text{O}/(\text{K}_2\text{O} + \text{Na}_2\text{O} + \text{CaO})$) also separate groups and show that the

TABLE 3. AVERAGE MINERAL COMPOSITIONS FOR INDIVIDUAL BASALT VESSEL SAMPLES

Pigeonite																					
Sample	N	SiO ₂	TiO ₂	Al ₂ O ₃	FeO	MnO	MgO	CaO	Na ₂ O	Total	Sample	N	SiO ₂	TiO ₂	Al ₂ O ₃	FeO	MnO	MgO	CaO	Na ₂ O	Total
ASH1	2	50.57	0.44	0.38	27.04	0.69	14.78	5.70	0.18	99.78	PET8	1	50.77	0.50	0.49	25.63	0.68	15.30	6.96	b.d.	100.33
ASH2	4	50.75	0.47	0.43	26.29	0.59	16.26	4.50	b.d.	99.29	PET15	1	50.94	0.56	0.51	26.55	0.90	15.30	5.26	b.d.	100.02
ASH4	5	51.12	0.54	0.57	25.09	0.67	16.55	5.29	0.10	99.93	RMB2	1	51.48	0.54	0.51	26.02	0.65	16.73	4.86	b.d.	100.79
ASH5	1	50.85	0.36	0.41	27.83	0.64	14.83	4.37	b.d.	99.29	RMB5	4	50.71	0.58	0.53	26.69	0.68	15.39	5.40	b.d.	99.98
ASH6	1	51.09	0.54	0.59	26.16	0.76	15.61	5.89	b.d.	100.64	RMB6	1	51.20	0.39	0.48	26.34	0.72	16.54	4.18	b.d.	99.85
ASH9	2	50.38	0.54	0.58	24.99	0.79	15.43	6.26	b.d.	98.97	RMB16	1	51.24	0.45	0.56	26.21	0.81	15.50	5.86	b.d.	100.63
ASH10	1	50.27	0.50	0.46	28.13	0.73	15.16	4.16	b.d.	99.41	RMB18	2	50.49	0.42	0.48	26.43	0.62	15.56	5.07	b.d.	99.07
ASH12	5	50.35	0.51	0.49	27.00	0.68	15.39	5.11	b.d.	99.53	RMB25	1	50.75	0.38	0.51	26.67	0.59	15.78	5.12	b.d.	99.80
BM1	1	51.00	0.55	0.70	24.86	0.57	16.44	5.59	b.d.	99.71	RMB26	1	49.74	b.d.	b.d.	31.81	0.83	12.56	3.75	b.d.	98.69
BM2	2	50.06	0.67	0.58	26.80	0.78	13.19	7.06	b.d.	99.14	RMB29	1	50.34	0.52	0.78	24.75	0.68	15.09	7.43	b.d.	99.59
BM5	1	50.43	0.41	0.41	26.05	0.62	15.09	5.69	0.30	99.00	RMB30	1	50.47	0.54	0.66	25.49	0.70	16.63	4.63	0.29	99.41
BRK5	2	50.58	0.45	0.33	27.94	0.68	15.51	4.36	b.d.	99.85	RMB32	1	50.49	0.49	0.50	26.69	0.57	15.86	4.09	b.d.	98.69
BRK6	1	50.62	0.61	0.49	27.05	0.74	15.47	5.08	b.d.	100.06	RMB33	2	50.28	0.40	0.43	26.76	0.61	15.86	4.59	0.35	99.28
FIT1	1	50.43	0.38	0.47	27.20	0.71	15.76	4.31	b.d.	99.26	RMB36	2	50.74	0.39	0.51	27.65	0.71	15.52	4.69	b.d.	100.21
FIT4	1	51.19	0.38	0.52	25.70	0.66	17.09	4.38	b.d.	99.92	RMB40	2	51.18	0.44	0.41	26.57	0.62	16.54	4.62	b.d.	100.38
MFA2	1	50.30	0.51	0.70	25.66	0.79	16.24	4.69	b.d.	98.89	ROM2	1	49.93	0.45	0.68	30.03	0.69	12.84	4.67	0.10	99.39
MFA3	2	50.94	0.47	0.41	26.73	0.78	14.75	5.84	0.18	100.10	ROM4	3	51.27	0.57	0.78	23.85	0.58	15.94	6.91	0.09	99.99
MFA4	1	50.42	0.53	0.56	26.49	0.69	15.07	5.11	b.d.	98.87	ROM6	1	50.68	0.42	0.55	28.35	0.74	14.45	5.24	0.09	100.54
MFA5	2	50.65	0.42	0.47	26.69	0.68	16.38	4.38	b.d.	99.67	ROM8	1	50.93	0.66	0.22	31.69	0.73	12.98	3.71	0.07	100.98
MFA8	2	50.43	0.51	0.85	23.96	0.59	15.08	7.33	b.d.	98.75	ROM9	1	51.83	0.37	0.50	25.53	0.64	17.02	4.31	0.06	100.26
MFA9	1	49.79	0.49	0.44	29.20	0.75	13.10	6.00	b.d.	99.77	ROM11	1	50.17	0.47	0.46	26.68	0.61	15.36	4.99	b.d.	98.74
MFA10	2	50.51	0.52	0.53	25.26	0.62	15.76	5.84	b.d.	99.04	ROM12	1	50.60	0.53	0.45	27.25	0.75	15.80	5.05	b.d.	100.42
PET1	6	50.60	0.50	0.53	25.80	0.74	15.15	6.12	0.13	99.57	ROM13	2	51.20	0.36	0.40	26.40	0.70	15.77	4.63	0.18	99.64
PET2	1	51.03	b.d.	b.d.	28.23	0.73	16.37	2.50	b.d.	98.86	ROM16	1	51.53	0.53	0.49	25.45	0.81	16.43	4.69	0.32	100.25
PET5	1	50.31	b.d.	0.31	27.97	0.57	15.43	3.98	b.d.	98.57	ROM18	1	50.74	0.35	0.49	26.71	0.82	16.18	4.79	b.d.	100.08
PET7	2	50.72	0.53	0.33	26.19	0.68	15.84	4.80	b.d.	99.09	ROM19	1	50.75	0.46	0.39	26.73	0.78	16.39	4.10	b.d.	99.60

Olivine															
Sample	N	SiO ₂	FeO	MnO	MgO	CaO	Total	Sample	N	SiO ₂	FeO	MnO	MgO	CaO	Total
RMB5	1	33.30	47.39	0.89	18.35	0.29	100.22	RMB5	1	33.30	47.39	0.89	18.35	0.29	100.22
ROM11	1	34.15	42.96	0.59	21.55	0.27	99.52	ROM11	1	34.15	42.96	0.59	21.55	0.27	99.52
ROM18	1	33.79	46.91	0.76	18.48	0.36	100.30	ROM18	1	33.79	46.91	0.76	18.48	0.36	100.30

Pigeonite was not analyzed in all samples. Raw data, calculation procedures, and standard deviations are given in Appendix 3 of Mallory (2000). Compositions are reported as wt.% oxides. N: number of analyses, N.A.: not analyzed, b.d.: below detection limit. Sample identification is as follows: Ashmolean Museum (ASH), British Museum (BM), Brooklyn Museum (BRK), Fitzwilliam Museum (FIT), Museum of Fine Arts, Boston (MFA), Petrie Museum of Archaeology (PET), Royal Museums of Art and History, Brussels (RMB), and Royal Ontario Museum (ROM).

vessel compositions plot with Haddadin averages (Figs. 4c, d).

COMPARING THE BASALT VESSELS TO THE BEDROCK SAMPLES

Variations in mineral composition in Egyptian basalts

By definition, only subalkaline basalts contain a low-Ca pyroxene. Orthopyroxene was not observed in any of the Egyptian basalt or vessel samples. However, pigeonite, though difficult to identify optically (it only occurs as small interstitial grains or as a thin rim on augite) was identified using the electron microprobe in Haddadin, Cairo–Suez and Middle Egypt basalts and in

about half of the vessels. Pigeonite was not identified in any of the Bahariya or southern Egypt samples of basalt. This is consistent with the basalts from southern Egypt and Bahariya suites being alkaline. The corollary is that the bedrock source(s) for vessels probably is(are) in northern Egypt.

Based on Al₂O₃ versus SiO₂ relationships in augite (Le Bas 1962), Egyptian basalts are variably alkaline, with southern Egypt basalts (W, L, and A) being most strongly alkaline, the Haddadin (H) flow and Bahariya Oasis (B), subalkaline, and Middle Egypt (M) and Cairo–Suez (C), transitional (Fig. 3a). Average compositions of augite in the vessels clearly indicate that these are subalkaline (Fig. 3b).

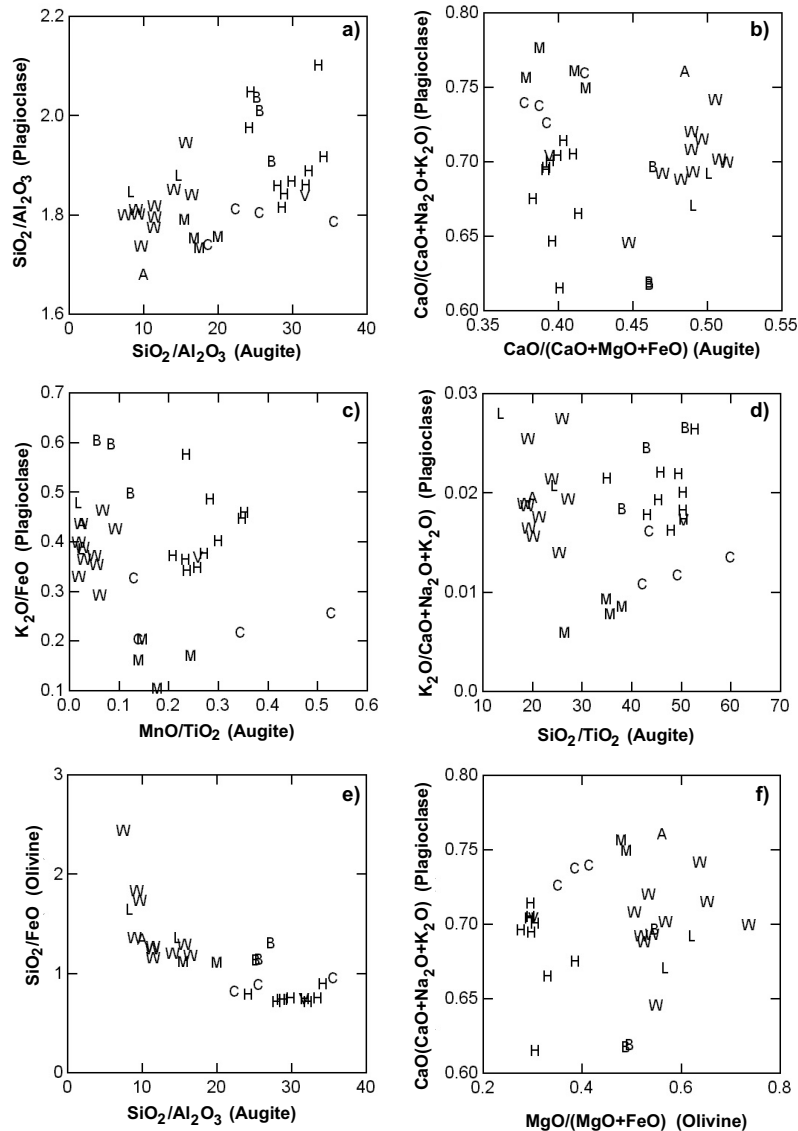


FIG. 4. Average values of ratios of constituents in augite plotted against those in plagioclase. a) $\text{SiO}_2/\text{Al}_2\text{O}_3$ in plagioclase shows a statistically significant positive correlation with $\text{SiO}_2/\text{Al}_2\text{O}_3$ in augite (correlation coefficient = 0.47 with $P = 0.004$). b) $\text{CaO}/(\text{CaO} + \text{MgO} + \text{FeO})$ of augite versus $\text{CaO}/(\text{CaO} + \text{Na}_2\text{O} + \text{K}_2\text{O})$ of plagioclase. c) The ratio MnO/TiO_2 in augite plotted against $\text{K}_2\text{O}/\text{FeO}$ of plagioclase. d) The $\text{SiO}_2/\text{TiO}_2$ value of augite versus $\text{K}_2\text{O}/(\text{CaO} + \text{Na}_2\text{O} + \text{K}_2\text{O})$ of plagioclase. e) The SiO_2/FeO value in olivine versus the $\text{SiO}_2/\text{Al}_2\text{O}_3$ value in augite. f) The value of $\text{CaO}/(\text{CaO} + \text{Na}_2\text{O} + \text{K}_2\text{O})$ of plagioclase plotted against $\text{MgO}/(\text{MgO} + \text{FeO})$ of olivine. For the vessels, the single datapoint represents the average of all 117 averages for the vessels. All ratios calculated from wt.% data, with total Fe as FeO. Symbols as in Figure 3. See text for discussion.

Two parameters that can be used to describe plagioclase [anorthite content = $\text{CaO}/(\text{CaO} + \text{Na}_2\text{O} + \text{K}_2\text{O})$, constituents in wt.%] and augite [wollastonite content =

$\text{CaO}/(\text{CaO} + \text{MgO} + \text{FeO})$, constituents in wt.%] compositions illustrate the utility of comparing mineral compositions (Fig. 4b). The alkaline, southern Egypt basalts,

useful for distinguishing groups (Tabachnick & Fidell 2001, p. 456-516). It creates arbitrary mathematical functions that separate data based on known groups. The bedrock samples were grouped by region (North, Middle, South) and flow or unit (Bahariya, Cairo–Suez Road, Haddadin, or Cairo–Suez Road, Haddadin, Middle Egypt). Grouping by region allows any vessels manufactured from Middle Egyptian basalts to be identified, and grouping by flow will identify the specific

basalt in Northern Egypt. Augite and plagioclase are abundant in all basalts and are, therefore, the two main minerals selected for comparison with the basalt vessels.

Clearly, the major elements in augite [(Ca,Mg,Fe²⁺, Al)₂(Si,Al)₂O₆] can help discriminate between regions and flows (Mallory-Greenough *et al.* 1999). As well, univariate F-statistics give probabilities for how correlated an element is with region or flow, and tend to rank the major elements higher than the minor elements. F-statistics ranked the constituents based on region (in descending order of probability, CaO, TiO₂, SiO₂, Al₂O₃, Na₂O, MgO, MnO, FeO) and by flow (in descending order, CaO, FeO, MnO, SiO₂, Na₂O, MgO, Al₂O₃, TiO₂). Therefore, these eight constituents were chosen for discriminant analysis of augite based on region and flow. Only two minor constituents (FeO, K₂O) in plagioclase [(Na,Ca)(Al,Si)₄O₈] were measured for this study. This fact and the restrictive nature of the crystal structure of plagioclase dictated that the major constituents SiO₂, Al₂O₃, CaO, and Na₂O be used for discrimination as well. Surprisingly, FeO was ranked lowest for correlation with both flow and region according to univariate F-statistics (region, K₂O, CaO, Na₂O, SiO₂, Al₂O₃, FeO; flow, Na₂O, CaO, SiO₂, K₂O, Al₂O₃, FeO). For pigeonite [(Mg,Fe²⁺,Ca)(Mg,Fe²⁺)Si₂O₆], like augite, the constituents SiO₂, TiO₂, Al₂O₃, FeO, MnO, MgO, CaO, and Na₂O were chosen. According to SYSTAT's univariate F-statistics, constituents selected for each mineral individually show highly significant correlations with the categorical variables, flow and region (P < 0.0001). Thus not surprisingly, the multivariate test statistics such as Wilks's Lambda, Pillai Trace, Hotelling–Lawley Trace, and Theta indicate that the element combinations chosen are also highly correlated (P < 0.0001) with region and flow (Tabachnick & Fidell 2001, p. 481).

Using unaveraged mineral compositions, the bedrock samples were correctly classified by region (North, Middle, South) using the discriminant functions 87% of the time for augite and 78% for plagioclase. Classification of northern flows (Bahariya, Cairo–Suez Road, Haddadin) was correct for 78% of augite, and 76% of plagioclase cases. Overlap, where it occurs, tends to be between Middle Egyptian and Cairo–Suez Road samples. Pigeonite was used to distinguish between Middle Egyptian, Cairo–Suez Road, and Haddadin basalts, and had a success rate in classification of 92%. Function scores for the mineral compositions, which are derived from the discriminant functions (Table 4) are plotted in Figures 6a, 6b, 7a, 7c, and 7e. Fields separating regions or flows were added manually and were based on the distribution of unaveraged data. For clarity, averaged data (Table 1, 3) are plotted in Figures 6 and 7. These useful diagrams summarize the degree of chemical variability of the minerals in Egyptian basalts and can be used to identify the source of the vessels.

The mineral data from the basalt vessels were averaged, and the average augite and plagioclase composi-

TABLE 4. EQUATIONS FOR CALCULATION OF FUNCTION SCORES

REGIONAL DISCRIMINATION-COEFFICIENTS ¹						
Function	Augite		Plagioclase			
	Function 1	Function 2	Function 1	Function 2		
SiO ₂	0.330	0.283	1.745		0.431	
TiO ₂	0.037	1.099				
Al ₂ O ₃	-0.154	1.157	-1.899		-0.326	
FeO	-0.263	0.649	-0.491		-2.107	
MnO	1.039	0.968				
MgO	0.083	1.111				
CaO	-0.899	0.009	1.874		-0.909	
Na ₂ O	-1.131	1.774	-2.784		-2.237	
K ₂ O			-7.616		1.438	
Constant	3.369	-43.503	-44.642		8.785	

FLOW DISCRIMINATION-COEFFICIENTS ²						
Function	Augite		Plagioclase		Pigeonite	
	1	2	1	2	1	2
SiO ₂	0.542	0.619	0.986	0.255	1.206	1.491
TiO ₂	-0.241	-2.293			0.687	7.019
Al ₂ O ₃	-1.127	1.054	-1.236	-1.725	1.097	2.085
FeO	-0.931	-1.603	1.990	0.247	0.208	0.368
MnO	-2.668	-1.455			1.352	-7.657
MgO	-1.576	-2.390			0.996	-0.714
CaO	-0.038	-2.250	2.095	4.313	-0.021	-0.622
Na ₂ O	2.280	2.046	-2.287	3.774	1.955	5.228
K ₂ O			2.821	12.771		
Constant	9.814	64.607	-33.474	-35.650	-86.385	-69.965

Function	FLOW DISCRIMINATION-COEFFICIENTS ³		ALKALINITY DISCRIMINATION-COEFFICIENTS ⁴	
	Function 1	Function 2	Function 1	Function 2
Augite SiO ₂	-0.405	1.725		
Augite TiO ₂	0.066	0.272	1.540	1.507
Augite FeO			0.230	0.789
Augite CaO	2.349	0.689	1.984	0.047
Plag. SiO ₂			-1.231	-0.894
Plag. Al ₂ O ₃			1.347	0.816
Plag. CaO	3.813	-2.363		
Plag. Na ₂ O	7.066	-4.083	5.289	2.350
Plag. K ₂ O	13.432	9.475		
Constant	-107.090	-56.420	-41.464	1.473

Function scores are calculated by multiplying the wt.% of each element oxide by its coefficient, summing the products, and adding the constant (e.g., plagioclase Regional Function 2 = (0.431*SiO₂) + (-0.326*Al₂O₃) + (-2.107*FeO) + (-0.909*CaO) + (-2.237*Na₂O) + (1.438*K₂O) + 8.785. Notes: 1: coefficients for Figure 6, 2: coefficients for Figure 7, 3: coefficients for Figure 8, and 4: coefficients for Figure 9.

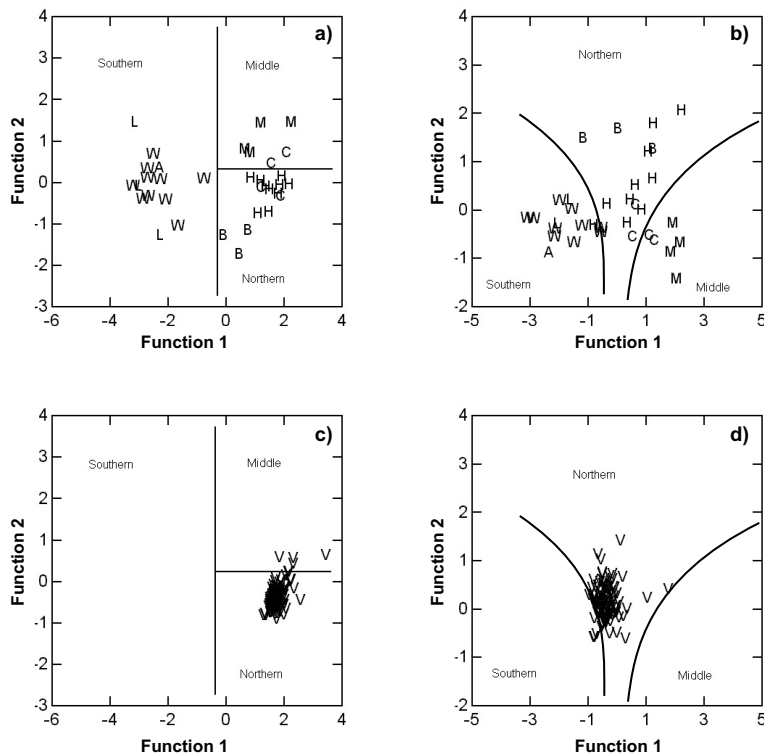


FIG. 6. Discrimination diagrams with which to discriminate among occurrences of basalt bedrock: a) regional, using augite, b) regional, plagioclase, c) vessels plotted on Figure 6a, and d) vessels plotted on Figure 6b. Fields were added on the basis of dominant region or flow using bedrock unaveraged individual compositions (Appendix 2, Mallory 2000). Average bedrock (Table 1) and vessel (Table 3) compositions are plotted for clarity. Function scores were calculated with the equations given in Table 4. Symbols as in Figure 3.

tions from the vessels (Table 3) were used with the discriminant functions (Table 4) to calculate function scores. When plotted on the regional diagrams derived from the bedrock samples, a Northern source is indicated (Figs. 6c, d). Using the Northern discriminant equations and plots, the Haddadin basalt is the most likely source for the basalt used in the vessels (Figs. 7b, d). The discriminant diagram using pigeonite (Fig. 7e), although based on fewer samples, also supports the Haddadin basalt as the source (Fig. 7f). Averages plotting outside the Northern or Haddadin fields belong to different vessel samples on each diagram, reflecting the statistical probability of variability and chemical variation within each region or flow.

Average compositions of augite and plagioclase for the bedrock samples were combined, and the constituents SiO_2 , TiO_2 , and CaO in augite and CaO , Na_2O , and K_2O in plagioclase used for discriminant analysis. Groups for separation were Bahariya, Cairo–Suez,

Haddadin, Middle Egypt, and Southern Egypt. These were separated with 100% efficiency. It was not possible to distinguish Wadi Natash, Lake Nasser and Gebel el Asr basalts from one another on this diagram (Fig. 8). The average of vessel averages was plotted, and as expected falls within the Haddadin field. It is important to note that even though mineral compositions for Haddadin and Cairo–Suez Road samples and the basalt vessels do overlap somewhat, the results of a study using the whole-rock composition of the same set of bedrock samples and a select few vessels eliminated the Cairo–Suez Road as a possible source for the artefacts (Greenough *et al.* 2001).

About half of the samples in the bedrock dataset are clearly tholeiitic (pigeonite-bearing), and the rest are alkaline basalts from southern Egypt. Bahariya is quite different from these two groups, and may be transitional in nature. Discriminant analysis based on alkalinity is extremely efficient at separating the basalts into three

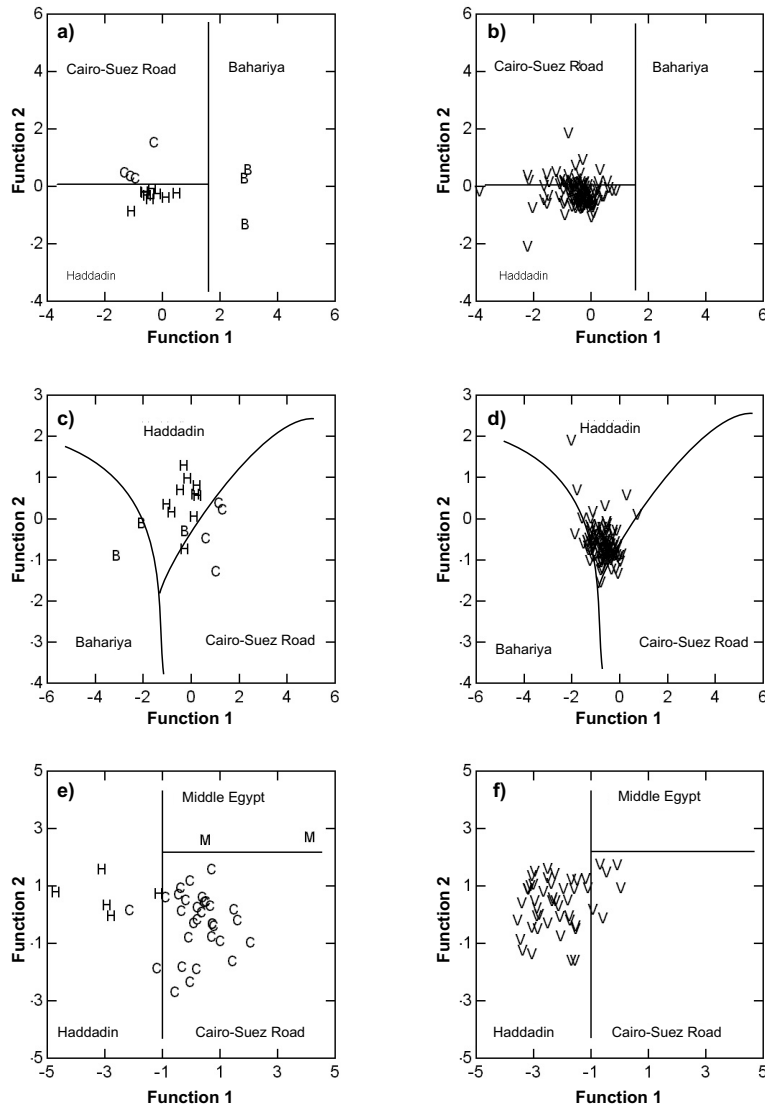


FIG. 7. Discrimination diagrams with which to discriminate among occurrences of basalt bedrock: a) northern flows, augite, c) northern flows, plagioclase, and e) flows, pigeonite. Vessels are plotted on b) augite (Fig. 7a), d) plagioclase (Fig. 7c), and f) pigeonite (Fig. 7e). Fields were determined using bedrock data as unaveraged individual compositions (Appendix 2, Mallory 2000) and are based on dominant region or flow. For clarity, bedrock (Table 1) and vessel (Table 3) averages are plotted. Function scores were calculated with the equations given in Table 4. Symbols as in Figure 3.

groups (subalkaline, transitional, and alkaline; Fig. 9) using TiO_2 , FeO and CaO in augite, and SiO_2 , Al_2O_3 , and Na_2O in plagioclase. The discriminant functions derived from Egyptian basalts were used to calculate scores for cursory examples of coexisting (same sample)

augite and plagioclase in MORB, continental and ocean-island tholeiites and an ocean-island alkali basalt (Fig. 9). The mineral-based alkalinity diagram correctly classified all of the "unknowns", suggesting that this approach to magma classification may have more widespread application.

ARCHEOLOGICAL IMPLICATIONS

There is no correlation between vessel provenance, age, or shape, and the source of the basalt used in their manufacture. The basalt in every vessel sampled and analyzed came from the same northern source, and most probably originated somewhere along the Haddadin basalt flow near modern Cairo. For the Predynastic Period, the site of Maadi (now a suburb of modern Cairo, see Fig. 1) may be the location of the vessel manufacturing industry. The site of this village is located about 15 km from an outcrop of Haddadin basalt (Mallory 2000, p. 96), and numerous repaired and reworked "factory seconds" were found in the settlement (Rizkana & Seeher 1988, p. 70). It is entirely possible that the knowledge and technical skills needed to manufacture basalt vessels were initially limited to this one site. Maadi was ideally situated at the apex of the Nile delta to control trade between Upper and Lower Egypt, and is considered one of the more important Predynastic trading centers (Hoffman 1990, p. 200-214). It is not surprising to discover that occupants of Maadi may have controlled the basalt vessel trade, and that the Upper (southern) Egyptian kings destroyed the settlement in their expansion northward.

A location for basalt vessel workshops has not been identified for the First Dynasty, and the raw material may have been shipped a considerable distance upstream to Hierakonpolis, where one group of stone ves-

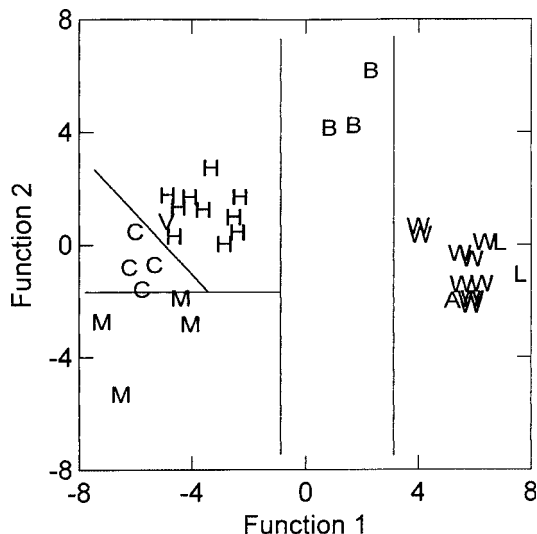


FIG. 8. Discrimination diagrams with which to discriminate among occurrences of basalt bedrock using combined average data on augite and plagioclase. Symbols as in Figure 3. Function scores were calculated using the data in Table 1, and the function coefficients in Table 4. Note divisions among groups can be tied to magma alkalinity.

sel craftsmen was located (Quibell & Green 1902, p. 17, pl. 68). Further excavation may reveal workshops at sites closer to the source. The widespread distribution of the artefacts and long life of the industry suggest that trade in these items was important locally and nationally long before Egypt was united, and for a considerable time after.

CONCLUSIONS

1. Results of electron-microprobe analyses confirm that augite is useful for distinguishing basalt units, but plagioclase, olivine and pigeonite may be just as helpful.
2. Major elements are as useful as trace elements in identifying bedrock units.
3. Although single-mineral discrimination diagrams efficiently distinguish Egyptian basalt units, diagrams based on mineral combinations appear more effective than single-mineral diagrams.

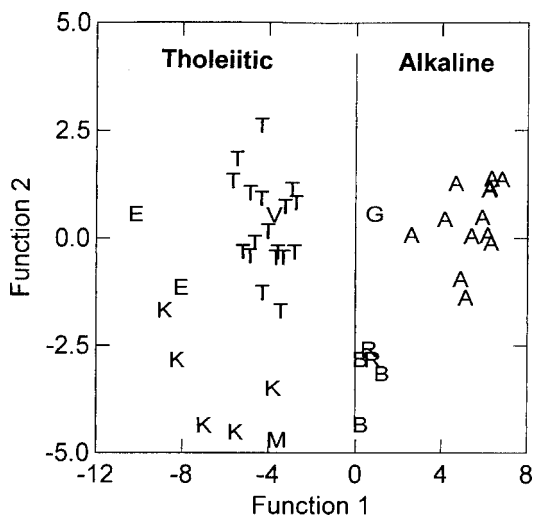


FIG. 9. Discrimination diagrams with which to discriminate among occurrences of basalt bedrock on the basis of alkalinity. Symbols: A: alkaline Egyptian basalts (Table 1), B: Bahariya (Table 1), E: Eastern North American Mesozoic basalts [Caraquet dyke, average of four compositions of augite and seven of plagioclase; Greenough & Papezik (1986); North Mountain basalt, upper unit: Papezik *et al.* (1988)], G: Gough Island [sample ALR61G; Le Roex (1985)], K: Kilauea [averages of samples EK4677, EK877, EK677, Easton & Garcia (1980); samples 2, 3, Ho & Garcia (1988)], M: MORB [East Pacific Rise, 02-01; Hekinian & Walker (1987)], R: Réunion Island [BO1942 and FI1956; Albarède & Tamagnan (1988)], T: tholeiitic Egyptian basalts (Table 1), V: vessels (Table 2). Function scores were generated using the data on Egyptian basalts (Table 1) and the function coefficients in Table 4.

4. A tholeiite – alkali basalt discrimination diagram constructed using the Egyptian basalt data and using a combination of plagioclase and augite data indicates that multi-mineral discrimination diagrams may be as effective as whole-rock diagrams for petrological discrimination.

5. A major advantage of mineral discrimination for archeology is that microsamples (0.001 g) provide enough material to definitively identify the bedrock source of valuable artefacts.

6. Mineral fingerprinting indicates that the 117 Predynastic Egyptian basalt vessels examined here were all produced from the Haddadin basalt in northern Egypt. Tradition has played an important role in the selection and use of stone in ancient Egypt, and may help explain why the Haddadin Basalt was used to manufacture artefacts for more than 1200 years. The discrimination diagrams summarize chemical variability in post-Jurassic Egyptian basalts and will allow future identifications of the source of basaltic Egyptian artefacts without collecting a bedrock database for comparison.

7. Maadi, the settlement closest to the Haddadin flow and richest in recycled “factory seconds”, probably controlled the vessel trade or workshops during the Predynastic period. These findings provide evidence that northern Egypt played an important role in the trade, economic and technological development of early (Predynastic) Egypt.

ACKNOWLEDGEMENTS

The Brooklyn Museum, Museum of Fine Arts (Boston), Royal Museums of Art and History (Brussels), Petrie Museum (London), Royal Ontario Museum (Toronto), Metropolitan Museum (New York), British Museum (London), Fitzwilliam Museum (Cambridge, U.K.), and Ashmolean Museum (Oxford) graciously allowed access to their collections. Basalt bedrock samples were contributed by J. Harrell, G. Franz, W. Crawford, The British Museum of Natural History (London), and N. Wassif. The authors appreciate the useful comments provided by J. Mungall and an anonymous reviewer. R. Corney drafted the diagrams. JDG and MPG acknowledge NSERC research grants.

REFERENCES

- ALBARÈDE, F. & TAMAGNAN, V. (1988): Modelling the recent geochemical evolution of the Piton de la Fournaise Volcano, Reunion Island, 1931–1986. *J. Petrol.* **29**, 997–1030.
- ALY, M.M., EL RAMLY, M.F. & KABESH, M.L. (compilers) (1983): *Analyses of Egyptian Rocks. 1. Igneous Rocks*. Geological Survey of Egypt and Mining Authority, Cairo, Egypt.
- ASTON, B.G. (1994): *Ancient Egyptian Stone Vessels: Materials and Forms*. Heidelberg Orientverlag, Heidelberg, Germany.
- AWADALLAH, M.F. (1980): Petrochemical and geochemical studies of the volcanic rocks of Bahariya Oasis, Western Desert, Egypt. *Ann. Geol. Surv. Egypt* **10**, 769–782.
- BORG, I.B. & GROENEN, P. (1987): *Modern Multidimensional Scaling: Theory and Application*. Springer Verlag, New York, N.Y.
- CRAWFORD, W.A., COULTER, D.H. & HUBBARD, B.H. (1984): The areal distribution, stratigraphy, and major element chemistry of the Wadi Natash volcanic series, Eastern Desert, Egypt. *J. Afr. Earth Sci.* **2**, 119–128.
- DE PUTTER, T. & KARLSHAUSEN, C. (1992): *Les pierres utilisées dans la sculpture et l'architecture de l'Égypte pharaonique*. Connaissance de l'Égypte Ancienne, Bruxelles, Belgique.
- EASTON, R.M. & GARCIA, M.O. (1980): Petrology of the Hilina Formation, Kilauea Volcano, Hawaii. *Bull. Volcanol.* **43**, 657–673.
- EL-HINNAWI, E.E. MAKSOU, M.A.A. (1968): Petrography of Cenozoic volcanic rocks of Egypt (UAR). *Geol. Rundsch.* **57**, 879–890.
- _____ & _____ (1972): Geochemistry of Egyptian Cenozoic basaltic rocks. *Chem. Erde* **31**, 93–112.
- FRANZ, G., PUCHELT, H. & PASTEELS, P. (1987): Petrology, geochemistry and age relations of Triassic and Tertiary volcanic rocks from SW Egypt and NW Sudan. *J. Afr. Earth Sci.* **6**, 335–352.
- GREENOUGH, J.D., GORTON, M.P. & MALLORY-GREENOUGH, L.M. (2001): The major- and trace-element whole-rock fingerprints of Egyptian basalts and the provenance of Egyptian artefacts. *Geoarchaeology* **16**, 763–784.
- _____, LONGERICH, H.P. & JACKSON, S.E. (1996): Trace element concentrations in wines by ICP–MS: evidence for the role of solubility in determining uptake by plants. *Can. J. Appl. Spectros.* **41**, 76–80.
- _____ & OWEN, J.V. (1998): Igneous layering in a dacite: on the origin and significance of Layer Cake Mountain, Kelowna, B.C., Canada. *Mineral. Mag.* **62**, 731–742.
- _____ & PAPEZIK, V.S. (1986): Petrology and geochemistry of the early Mesozoic Caraquet dyke, New Brunswick, Canada. *Can. J. Earth Sci.* **23**, 193–201.
- HARRELL, J.A. & BOWN, T.M. (1995): An Old Kingdom basalt quarry at Widan el-Faras and the quarry road to Lake Moeris. *J. Am. Research Center in Egypt* **32**, 71–91.
- HEKINIAN, R. & WALKER, D. (1987): Diversity and spatial zonation of volcanic rocks from the East Pacific Rise near 21°N. *Contrib. Mineral. Petrol.* **96**, 265–280.

- HO, R.A. & GARCIA, M.O. (1988): Origin of differentiated lavas at Kilauea Volcano, Hawaii: implications from the 1955 eruption. *Bull. Volcanol.* **50**, 35-46.
- HOFFMAN, M.A. (1990): *Egypt Before the Pharaohs*. Dorset Press, New York, N.Y.
- HUBBARD, H.B. (1977): *Geochemical Evolution of the Wadi Natash Volcanic Field, an Alkaline Basalt Flood in the Eastern Desert of Egypt*. M.Sc. thesis, Univ. of South Carolina, Columbia, South Carolina.
- _____, WOOD, L.F. & ROGERS, J.J.W. (1987): Possible hydration anomaly in the upper mantle prior to Red Sea rifting: evidence from petrologic modelling of the Wadi Natash alkali basalt sequence of eastern Egypt. *Geol. Soc. Am. Bull.* **98**, 92-98.
- HUTH, A. & FRANZ, G. (1988): Structural development of the Precambrian basement in the Bir Safsaf – Aswân area, SW-Egypt. *Geol. Rundsch.* **77**, 439-451.
- IRVINE, T.N. & BARAGAR, W.R.A. (1971): A guide to the chemical classification of common volcanic rocks. *Can. J. Earth Sci.* **8**, 523-548.
- KLEMM, R. & KLEMM D.D. (1993): *Steine und Steinbrüche im alten Ägypten*. Springer-Verlag, Berlin, Germany.
- LE BAS, M.J. (1962): The role of aluminum in igneous clinopyroxenes with relation to their parentage. *Am. J. Sci.* **260**, 267-288.
- LE ROEX, A.P. (1985): Geochemistry, mineralogy and magmatic evolution of the basaltic and trachytic lavas from Gough Island, South Atlantic. *J. Petrol.* **26**, 149-186.
- LETERRIER, J., MAURY, R.C., THONON, P., GIRARD, D. & MARCHAL, M. (1982): Clinopyroxene composition as a method of identification of the magmatic affinities of paleo-volcanic series. *Earth Planet. Sci. Lett.* **59**, 139-154.
- LOTFY, H.I., VAN DER VOO, R., HALL, C.M., KAMEL, O.A. & ABDEL AAL, A.Y. (1995): Paleomagnetism of Early Miocene basaltic eruptions in the areas east and west of Cairo. *J. Afr. Earth Sci.* **21**, 407-419.
- LUCAS, A. (1930): Egyptian Predynastic stone vessels. *J. Egyptian Archaeol.* **16**, 200-212.
- MALLORY, L.M. (2000): *Predynastic and First Dynasty Egyptian Basalt Vessels*. Ph.D. thesis, Univ. of Toronto, Toronto, Canada.
- MALLORY-GREENOUGH, L.M., GREENOUGH, J.D. & OWEN, J.V. (1998): New data for old pots: trace-element characterization of Ancient Egyptian pottery using ICP-MS. *J. Archaeol. Sci.* **25**, 85-97.
- _____, _____ & _____ (1999): The stone source of Predynastic basalt vessels: mineralogical evidence for quarries in northern Egypt. *J. Archaeol. Sci.* **26**, 1261-1272.
- _____, _____ & _____ (2000): The origin and use of basalt in Old Kingdom funerary temples. *Geoarchaeol.* **15**, 315-330.
- MAYNARD, J.B. (1984): Composition of plagioclase feldspar in modern deep-sea sands: relationship to tectonic setting. *Sedimentol.* **31**, 493-501.
- MENEISY, M.Y. (1990): Vulcanicity. In *The Geology of Egypt* (R. Said, ed.). A.A. Balkema, Rotterdam, The Netherlands (157-172).
- NISBET, E.G. & PEARCE J.A. (1977): Clinopyroxene composition in mafic lavas from different tectonic settings. *Contrib. Mineral. Petrol.* **63**, 149-160.
- PAPEZIK, V.S., GREENOUGH, J.D., COLWELL, J.A., & MALLINSON, T.J. (1988): North Mountain basalt from Digby, Nova Scotia: models for a fissure eruption from stratigraphy and petrochemistry. *Can. J. Earth Sci.* **25**, 74-83.
- PEARCE, J.A. (1996): A user's guide to basalt discrimination diagrams. In *Trace Element Geochemistry of Volcanic Rocks: Applications for Massive Sulphide Exploration* (D.A. Wyman, ed.). *Geol. Assoc. Can., Short Course Notes* **12**, 79-113.
- _____, & CANN, J.R. (1973): Tectonic setting of basic volcanic rocks determined using trace element analyses. *Earth Planet. Sci. Lett.* **19**, 290-300.
- PETRIE, W.M.F. (1900): *The Royal Tombs of the First Dynasty I*. Egypt Exploration Fund, London, U.K.
- _____, (1901a): *The Royal Tombs of the Earliest Dynasties II*. Egypt Exploration Fund, London, U.K.
- _____, (1901b): *The Royal Tombs of the Earliest Dynasties II - Extra Plates*. Egypt Exploration Fund, London, U.K.
- _____, (1937): *Stone and Metal Vases*. British School of Archaeology in Egypt, London, U.K.
- PHILPOTTS, A.R. (1990): *Principles of Igneous and Metamorphic Petrology*. Prentice Hall, Englewood Cliffs, N.J.
- PORAT, N. & SEEHER, J. (1988): Petrographic analyses of pottery and basalt from Predynastic Maadi. *Mitt. Deutsch. Archäol. Inst., Abt. Kairo* **44**, 215-228.
- QUIBELL, J.E. & GREEN, F.W. (1902): *Hierakonpolis II*. Bernard Quaritch, London, U.K.
- RESSETAR, R. & MONRAD, J.R. (1983): Chemical composition and tectonic setting of the Dokhan Volcanic Formation, Eastern Desert, Egypt. *J. Afr. Earth Sci.* **1**(2), 103-112.
- RIZKANA, I. & SEEHER, J. (1988): *Maadi II: The Lithic Industries of the Predynastic Settlement*. Philipp von Zabern, Mainz, Germany.
- SAID, R. (1962): *The Geology of Egypt*. Elsevier, New York, N.Y.

- _____ & MARTIN, L. (1964): Cairo area geological excursion notes. In *Guidebook to the Geology and Archaeology of Egypt* (F.A. Reilly, ed.). Petroleum Exploration Society of Libya, 6th Annual Field Conf., Cairo, Egypt (107-121).
- SCHELSTRAETE, V. (1998): *Petrologische studie van stenen vaatwerk uit de Koningsgraven van de 1ste en 2de dynastie te Umm el-Qaab (Abydos), Boyen-Egypte*. M.A. thesis, Ghent Univ., Ghent, Holland.
- TABACHNIK, B.G. & FIDELL, L.S. (2001): *Using Multivariate Statistics*. Allyn and Bacon, New York, N.Y.
- TEGNER, C. (1997): Iron in plagioclase as a monitor of the differentiation of the Skaergaard intrusion. *Contrib. Mineral. Petrol.* **128**, 45-51.
- VON DER WAY, T. (1993) *Untersuchungen zur Spätvor- und Frühgeschichte Unterägyptens*. Heidelberger Orientverlag, Heidelberg, Germany.
- WASSIF, N.A. (1986): Magnetic mineralogy of basalts from El-Bahnasa and Tahna, Egypt. *J. Geophys.* **60**, 47-55.
- WILKINSON, L., HILL, M., WELNA, J.P. & BIRKENBEUEL, G.K. (1992): *SYSTAT for Windows: Statistics, Version 5 Edition*. SYSTAT Inc., Evanston, Illinois.
- WILLIAMS, D.F. (1983): Petrology of ceramics. In *The Petrology of Archaeological Artefacts* (D.R.C. Kempe & A.P. Harvey, eds.). Oxford University Press, Oxford, U.K. (301-329).
- WINCHESTER, J.A. & FLOYD, P.A. (1977): Geochemical discrimination of different magma series and their differentiation products using immobile elements. *Chem. Geol.* **20**, 325-343.

Received March 25, 2001, revised manuscript accepted May 1, 2002.

APPENDIX



FIG. A1. This is the preserved upper part of a First Dynasty beaker (accession number E4839; RMB2) excavated at Abydos early in the 20th century by W.M.F. Petrie. Reproduced courtesy of the Royal Museums of Art and History, Brussels, Belgium.



FIG. A2. A unique, unprovenanced Predynastic vessel (accession number E2326; RMB34) with inlaid ivory eyes placed beside the jar's handle to create an owl's face. This jar is 34.8 cm tall. Reproduced courtesy of the Royal Museums of Art and History, Brussels, Belgium.



FIG. A3. Two Predynastic tubular-handled vessels from Gerzeh found by E. Wainwright in 1910. The jar on the left (accession number E3373; RMB4) was found in an intact tomb, whereas the other's (accession number E3372; RMB5) had been robbed in antiquity. Vessel heights are 11.1 cm (left) and 5.4 cm (right). Reproduced courtesy of the Royal Museums of Art and History, Brussels, Belgium.



FIG. A4. Discovered in the looted First Dynasty of King Djer at Abydos by W.M.F. Petrie, this bowl (accession number EA458; RMB20) has been reconstructed from fragments. It is approximately 6.3 cm high and 14.4 cm wide at the rim. Reproduced courtesy of the Royal Museums of Art and History, Brussels, Belgium.